

<https://helda.helsinki.fi>

Search for a heavy pseudoscalar boson decaying to a Z and a Higgs boson at root s=13TeV

The CMS collaboration

2019-07-03

The CMS Collaboration , Sirunyan , A M , Tumasyan , A , Eerola , P , Kirschenmann , H , Pekkanen , J , Voutilainen , M , Havukainen , J , Heikkilä , J K , Jarvinen , T , Karimäki , V , Kinnunen , R , Lampen , T , Lassila-Perini , K , Laurila , S , Lehti , S , Linden , T , Luukka , P , Mäenpää , T , Siikonen , H , Tuominen , E , Tuominiemi , J & Tuuva , T 2019 , ' Search for a heavy pseudoscalar boson decaying to a Z and a Higgs boson at root s=13TeV ' , European Physical Journal C. Particles and Fields , vol. 79 , no. 7 , 564 . <https://doi.org/10.1140/epjc/s10052-019-7058-z>

<http://hdl.handle.net/10138/311596>

<https://doi.org/10.1140/epjc/s10052-019-7058-z>

cc_by

publishedVersion

Downloaded from Helda, University of Helsinki institutional repository.

This is an electronic reprint of the original article.

This reprint may differ from the original in pagination and typographic detail.

Please cite the original version.



Search for a heavy pseudoscalar boson decaying to a Z and a Higgs boson at $\sqrt{s} = 13$ TeV

CMS Collaboration*

CERN, 1211 Geneva 23, Switzerland

Received: 3 March 2019 / Accepted: 18 June 2019 / Published online: 3 July 2019
© CERN for the benefit of the CMS collaboration 2019

Abstract A search is presented for a heavy pseudoscalar boson A decaying to a Z boson and a Higgs boson with mass of 125 GeV. In the final state considered, the Higgs boson decays to a bottom quark and antiquark, and the Z boson decays either into a pair of electrons, muons, or neutrinos. The analysis is performed using a data sample corresponding to an integrated luminosity of 35.9 fb^{-1} collected in 2016 by the CMS experiment at the LHC from proton–proton collisions at a center-of-mass energy of 13 TeV. The data are found to be consistent with the background expectations. Exclusion limits are set in the context of two-Higgs-doublet models in the A boson mass range between 225 and 1000 GeV.

1 Introduction

The discovery of a Higgs boson at the CERN LHC [1,2] and the measurement of its mass, spin, parity, and couplings [3,4] raises the question of whether the Higgs boson sector consists of only one scalar doublet, which results in a single physical Higgs boson as expected in the standard model (SM), or whether additional bosons are involved in electroweak (EW) symmetry breaking.

The two-Higgs-doublet model (2HDM) [5] provides an extension of the SM Higgs boson sector introducing a second scalar doublet. The 2HDM is incorporated in supersymmetric models [6], axion models [7], and may introduce additional sources of explicit or spontaneous CP violation that explain the baryon asymmetry of the universe [8]. Various formulations of the 2HDM predict different couplings of the two doublets to right-handed quarks and charged leptons: in the Type-I formulation, all fermions couple to only one Higgs doublet; in the Type-II formulation, the up-type quarks couple to a different doublet than the down-type quarks and leptons; in the “lepton-specific” formulation, the quarks couple to one of the Higgs doublets and the leptons couple to the other; and in the “flipped” formulation, the up-type fermions

and leptons couple to one of the Higgs doublets, while the down-type quarks couple to the other.

The two Higgs doublets entail the presence of five physical states: two neutral and CP -even bosons (h and H , the latter being more massive), a neutral and CP -odd boson (A), and two charged scalar bosons (H^\pm). The model has two free parameters, α and $\tan \beta$, which are the mixing angle and the ratio of the vacuum expectation values of the two Higgs doublets, respectively. If $\tan \beta \lesssim 5$, the dominant A boson production process is via gluon–gluon fusion, otherwise associated production with a b quark–antiquark pair becomes significant. The diagrams of the two production modes are shown in Fig. 1. At small $\tan \beta$ values the heavy pseudoscalar boson A may decay with a large branching fraction to a Z and an h boson, if kinematically allowed [5]. These models can be probed either with indirect searches, by measuring the cross section and couplings of the SM Higgs boson [9], or by performing a direct search for an A boson.

This paper describes a search for a heavy pseudoscalar A boson that decays to a Z and an h boson, both on-shell, with the Z boson decaying to $\ell^+ \ell^-$ (ℓ being an electron or a muon) or to a pair of neutrinos, and the h boson to $b\bar{b}$. The h boson is assumed to be the 125 GeV boson discovered at the LHC. In this search, the candidate A boson is reconstructed from the invariant mass of the visible decay products in events when the Z boson decays to charged leptons, or is inferred through a partial reconstruction of the mass using quantities measured in the transverse plane when the Z boson decays to neutrinos. The signal would emerge as a peak above the SM continuum of the four-body invariant mass (m_{Zh}) spectrum for the former decay mode and the transverse mass (m_{Zh}^T) for the latter. The signal sensitivity is maximized by exploiting the known value of the h boson mass to rescale the jet momenta and significantly improve the m_{Zh} resolution. In addition, selections based on multivariate discriminators, exploiting event variables such as angular distributions, are used to optimize the signal efficiency and background rejection. This search is particularly sensitive to a pseudoscalar A boson with a mass smaller than twice the top quark mass and for small

* e-mail: cms-publication-committee-chair@cern.ch

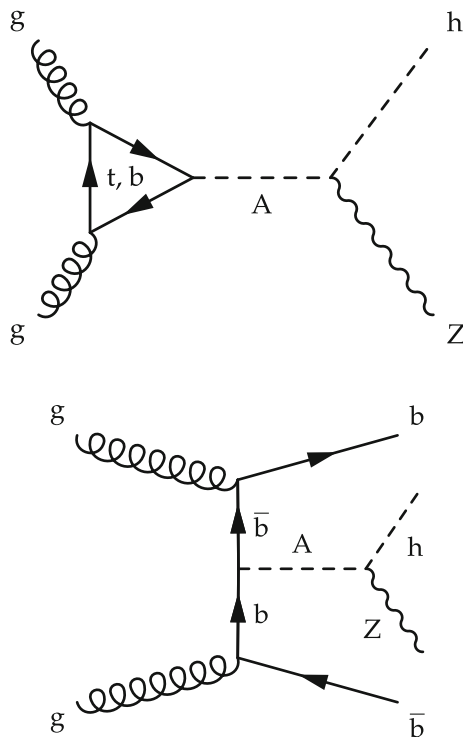


Fig. 1 Representative Feynman diagrams of the production in the 2HDM of a pseudoscalar A boson via gluon–gluon fusion (upper) and in association with b quarks (lower)

$\tan \beta$ values. In this region of the 2HDM parameter space, the A boson cross section is larger than 1 pb, and the A boson decays predominantly to Zh [5].

With respect to the CMS search performed at $\sqrt{s} = 8$ TeV [10], this analysis benefits from the increased center-of-mass energy and integrated luminosity, includes final states with invisible decays of the Z boson, increases the sensitivity to b quark associated production, and extends the A boson mass (m_A) range from 600 to 1000 GeV. At larger m_A , the angular separation between the b quarks becomes small, and the Higgs boson is reconstructed as a single large-cone jet; the corresponding CMS analysis presents limits on the 2HDM from 800 GeV to 2 TeV [11]. The ATLAS Collaboration has published a search probing Zh resonances with similar event selections based on a comparable data set, observing a mild excess near 440 GeV in categories with additional b quarks [12].

2 The CMS detector

A detailed description of the CMS detector, together with a definition of the coordinate system used and the relevant kinematic variables, can be found in Ref. [13].

The central feature of the CMS apparatus is a superconducting solenoid of 6 m internal diameter, providing a mag-

netic field of 3.8 T. Within the solenoid volume are a silicon pixel and strip tracker, a lead tungstate crystal electromagnetic calorimeter (ECAL), and a brass and scintillator hadron calorimeter (HCAL), each composed of a barrel and two endcap sections. Forward calorimeters extend the pseudorapidity coverage provided by the barrel and endcap detectors. Muons are detected in gas-ionization chambers embedded in the steel flux-return yoke outside the solenoid.

The silicon tracker measures charged particles within the pseudorapidity range $|\eta| < 2.5$. It consists of 1440 silicon pixel and 15,148 silicon strip detector modules. For nonisolated particles with transverse momenta of $1 < p_T < 10$ GeV and $|\eta| < 1.4$, the track resolutions are typically 1.5% in p_T and 25–90 (45–150) μm in the transverse (longitudinal) impact parameter [14]. The ECAL provides coverage up to $|\eta| < 3.0$, and the energy resolution for unconverted or late-converting electrons and photons in the barrel section is about 1% for particles that have energies in the range of tens of GeV. The dielectron mass resolution for $Z \rightarrow e^+e^-$ decays when both electrons are in the ECAL barrel is 1.9%, and is 2.9% when both electrons are in the endcaps [15]. The muon detectors covering the range $|\eta| < 2.4$ make use of three different technologies: drift tubes, cathode strip chambers, and resistive-plate chambers. Combining muon tracks with matching tracks measured in the silicon tracker results in a p_T resolution of 2–10% for muons with $0.1 < p_T < 1$ TeV [16].

The first level of the CMS trigger system [17], composed of custom hardware processors, uses information from the calorimeters and muon detectors to select the most interesting events in a fixed time interval of less than 4 μs . The high-level trigger (HLT) processor farm decreases the event rate from around 100 kHz to about 1 kHz, before data storage.

3 Event reconstruction

A global event reconstruction is performed with a particle-flow (PF) algorithm [18], which uses an optimized combination of information from the various elements of the detector to identify stable particles reconstructed in the detector as an electron, a muon, a photon, a charged or a neutral hadron. The PF particles have to pass the charged-hadron subtraction (CHS) algorithm [19], which discards charged hadrons not originating from the primary vertex, depending on the longitudinal impact parameter of the track. The primary vertex is selected as the vertex with the largest value of summed p_T^2 of the PF particles, including charged leptons, neutral and charged hadrons clustered in jets, and the associated missing transverse momentum \vec{p}_T^{miss} , which is the negative vector sum of the \vec{p}_T of those jets.

Electrons are reconstructed in the fiducial region $|\eta| < 2.5$ by matching the energy deposits in the ECAL with charged particle trajectories reconstructed in the tracker [15]. The electron identification is based on the distribution of energy deposited along the electron trajectory, the direction and momentum of the track, and its compatibility with the primary vertex of the event. Electrons are further required to be isolated from other energy deposits in the detector. The electron relative isolation parameter is defined as the sum of transverse momenta of all the PF candidates, excluding the electron itself, divided by the electron p_T . The PF candidates are considered if they lie within $\Delta R = \sqrt{(\Delta\eta)^2 + (\Delta\phi)^2} < 0.3$ around the electron direction, where ϕ is the azimuthal angle in radians, and after the contributions from pileup and other reconstructed electrons are removed [15].

Muons are reconstructed within the acceptance of the CMS muon systems using tracks reconstructed in both the muon spectrometer and the silicon tracker [16]. Additional requirements are based on the compatibility of the trajectory with the primary vertex, and on the number of hits observed in the tracker and muon systems. Similarly to electrons, muons are required to be isolated. The muon isolation is computed from reconstructed PF candidates within a cone of $\Delta R < 0.4$ around the muon direction, ignoring the candidate muon, and divided by the muon p_T [16].

Hadronically decaying τ leptons are used to reject $W \rightarrow \tau\nu$ background events, and are reconstructed by combining one or three hadronic charged PF candidates with up to two neutral pions, the latter also reconstructed by the PF algorithm from the photons arising from the $\pi^0 \rightarrow \gamma\gamma$ decay [20].

Jets are clustered using the anti- k_T algorithm [21, 22] with a distance parameter of 0.4. The contribution of neutral particles originating from pileup interactions is estimated to be proportional to the jet area derived using the FASTJET package [22, 23], and subtracted from the jet energy. Jet energy corrections, extracted from both simulation and data in multijet, γ +jets, and Z+jets events, are applied as functions of the p_T and η of the jet to correct the jet response and to account for residual differences between data and simulation. The jet energy resolution amounts typically to 15–20% at 30 GeV, 10% at 100 GeV, and 5% at 1 TeV [24].

Jets that originate from b quarks are identified with a combined secondary vertex b-tagging algorithm [25] that uses the tracks and secondary vertices associated with the jets as inputs to a neural network. The algorithm provides a b jet tagging efficiency of 70%, and a misidentification rate in a sample of quark and gluon jets of about 1%. The b tagging efficiency is corrected to take into account a difference at the few percent level in algorithm performance for data and simulation [25].

4 Data and simulated samples

The data sample analyzed in this search corresponds to an integrated luminosity of 35.9 fb^{-1} of proton–proton (pp) collisions at a center-of-mass energy of 13 TeV collected with the CMS detector at the LHC. Data are collected using triggers that require either the presence of at least one isolated electron or isolated muon with $p_T > 27 \text{ GeV}$, or alternatively a p_T^{miss} or H_T^{miss} larger than 90–110 GeV, the value depending on the instantaneous luminosity. The p_T^{miss} is the magnitude of \vec{p}_T^{miss} , and H_T^{miss} is defined as the momentum imbalance of the jets in the transverse plane [17].

The pseudoscalar boson signal is simulated at leading order (LO) with the MADGRAPH5_aMC@NLO 2.2.2 matrix element generator [26] in both the gluon–gluon fusion and b quark associated production modes according to the 2HDM [5], assuming a narrow signal width. The h boson mass is set to 125 GeV, and the A boson mass ranges between 225 and 1000 GeV. The $A \rightarrow Z\text{h}$ decay is simulated with MADSPIN [27]. The Higgs boson is forced to decay to $b\bar{b}$, and the vector boson to a pair of electrons, muons, τ leptons, or neutrinos. In the gluon–gluon fusion production mode, up to one additional jet is included in matrix element calculations, and only the top quark contributes to the loop shown in Fig. 1 (upper). The 2HDM cross sections and branching fractions are computed at next-to-next-to-leading order (NNLO) with 2HDMC 1.7.0 [28] and SUSHi 1.6.1 [29], respectively. The parameters used in the models are: $m_h = 125 \text{ GeV}$, $m_H = m_{H^\pm} = m_A$, the discrete Z_2 symmetry is broken as in the minimal supersymmetric standard model (MSSM), and CP is conserved at tree level in the 2HDM Higgs sector [5]. The branching fractions of the Z boson are taken from the measured values [30].

The SM backgrounds in this search consist of the inclusive production of a vector boson in association with other jets (V+jets, with $V = W$ or Z , and V decaying to final states with charged leptons and neutrinos), and top quark pair production ($t\bar{t}$). V+jets events are simulated at LO with MADGRAPH5_aMC@NLO with up to four partons included in the matrix element calculations and using the MLM matching scheme [31]. The event yield is normalized to the NNLO cross section computed with FEWZ v3.1 [32]. The V boson p_T spectra are corrected to account for next-to-leading order (NLO) quantum chromodynamics (QCD) and EW contributions [33]. The $t\bar{t}$ and single top quark in the t channel and tW production are simulated at NLO with POWHEG v2 generator [34–36]. The number of events for the top quark pair production process is rescaled according to the cross section computed with TOP++ v2.0 [37] at NNLO+NNLL, and the transverse momenta of top quarks are corrected to match the distribution observed in data [38]. Other SM processes, such as SM vector boson pair production (VV), SM Higgs boson production in association with a vector boson (Vh),

single top quark ($t + X$) production in the s channel, and top quark production in association with vector bosons, are simulated at NLO in QCD with MADGRAPH5_aMC@NLO using the FxFX merging scheme [39]. The multijet contribution, estimated with the use of samples generated at LO with the same generator, is negligible after analysis selections.

All the simulated processes use the NNPDF 3.0 [40] parton distribution functions (PDFs), and are interfaced with PYTHIA 8.205 [41,42] for the parton showering and hadronization. The CUETP8M1 underlying event tune [43] is used in all samples, except for top quark pair production, which adopts the CUETP8M2T4 tune [44].

Additional minimum bias pp interactions within the same or adjacent bunch crossings (pileup) are added to the simulated processes, and events are weighted to match the observed average number of interactions per bunch crossing. Generated events are processed through a full CMS detector simulation based on GEANT4 [45] and reconstructed with the same algorithms used for collision data.

5 Event selection

Events are classified into three independent categories (0ℓ , $2e$, and 2μ), based on the number and flavor of the reconstructed leptons. Events are required to have at least two jets with $p_T > 30$ GeV and $|\eta| < 2.4$ to be suitable candidates for the reconstruction of the $h \rightarrow b\bar{b}$ decay. If more than two jets fulfill the requirements, the ones with the largest b tagging discriminator value are used to reconstruct the Higgs boson candidate. The efficiency of the correct assignment of the reconstructed jets to initial quarks originating from the Higgs boson decay varies between 80 and 97%, after applying the event selections, depending on the category and final state.

In the 0ℓ category, no isolated electron or muon with $p_T > 10$ GeV is allowed. Events containing isolated hadronic decays of the τ leptons with $p_T > 18$ GeV are vetoed as well. A selection is applied on the reconstructed p_T^{miss} , which is required to be larger than 200 GeV, such that the p_T^{miss} trigger is at least 95% efficient. In order to select a topology where the Z boson recoils against the Higgs boson, a Lorentz boost requirement of 200 GeV on the p_T of the Higgs boson candidate, p_T^{bb} , is applied.

Multijet production is suppressed by requiring that the minimum azimuthal angular separation between all jets and the missing transverse momentum vector must satisfy $\Delta\phi(\text{jet}, \vec{p}_T^{\text{miss}}) > 0.4$. The multijet simulation is validated in a region obtained by inverting the $\Delta\phi$ selection, finding a good description of data. When the Z boson decays to neutrinos, the resonance mass m_A cannot be reconstructed directly. In this case, m_A is estimated by computing the transverse mass from the \vec{p}_T^{miss} and the four-momenta of the two

jets used to reconstruct the Higgs boson candidate, defined as $m_{Z\text{h}}^T = \sqrt{2p_T^{\text{miss}} p_T^{\text{h}} [1 - \cos \Delta\phi(\text{h}, \vec{p}_T^{\text{miss}})]}$, which has to be larger than 500 GeV. The efficiency of these selections for signal events with $m_A \lesssim 500$ GeV is small, because the p_T of the Z boson is not sufficient to produce a p_T^{miss} large enough to pass the selection; thus, the contribution of the 0ℓ category is significant only for large m_A .

In the $2e$ and 2μ categories, events are required to have at least two isolated electrons or muons within the detector geometrical acceptance. The p_T threshold on the lepton is referred to as p_T^ℓ , and is set to 30 GeV for the lepton with highest p_T , and to 10 GeV for the lepton with next-highest p_T . The Z boson candidate is formed from the two highest p_T , opposite charge, same-flavor leptons, and must have an invariant mass $m_{\ell\ell}$ between 70 and 110 GeV. The $m_{\ell\ell}$ selection lowers the contamination from $t\bar{t}$ dileptonic decays, and significantly reduces the contribution from $Z \rightarrow \tau\tau$ decays. The reconstructed p_T^{miss} also has to be smaller than 100 GeV to reject the $t\bar{t}$ background. In order to maximize the signal acceptance, no Lorentz boost requirement is applied to the Z and h boson candidates in the dileptonic categories. The A boson candidate is reconstructed from the invariant mass $m_{Z\text{h}}$ of the Z and h boson candidates.

If the two jets originate from a Higgs boson, their invariant mass is expected to peak close to 125 GeV. Events with a dijet invariant mass m_{jj} between 100 and 140 GeV enter the signal regions (SRs); otherwise, if $m_{jj} < 400$ GeV, they fall in dijet mass sidebands, which are used as control regions (CRs) to estimate the contributions of the main backgrounds. Signal regions are further divided by the number of jets passing the b tagging requirement (1, 2, or at least 3 b tags). The 3 b tag category has been defined to select the additional b quarks from b quark associated production. In this region, at least one additional jet, other than the two used to reconstruct the h boson, has to pass the kinematic selections and b tagging requirements. The fraction of signal events passing the m_{jj} selection in the SR is 66–82% and 45–65% in the 1 and 2 b tag categories, respectively. Control regions for the Z+jets background share the same selections as the corresponding SR, except for the m_{jj} mass window.

Dedicated CRs are defined to estimate the $t\bar{t}$ and W+jets backgrounds, which may enter the 0ℓ SR if the lepton originating from the W decay is outside the detector geometrical acceptance or is not reconstructed. Two W+jets CRs share the same selection as in the 0ℓ categories, but require exactly one electron or one muon passing the same trigger and selections of the leading lepton in the 2ℓ categories. In order to mimic the kinematics of leptonic W decays, where the lepton is outside the geometrical acceptance or is not reconstructed in the detector, the p_T^{miss} is recalculated by removing the contribution of the lepton. The $\min(\Delta\phi)$ requirement is removed, and the dijet invariant mass selection is not applied, as the

signal is absent in 1ℓ final states. Events are required to have three or fewer jets, none of them b tagged, to reduce the $t\bar{t}$ contribution.

Four different CRs associated with the production of events containing top quarks are defined by inverting specific selections with respect to the SR definition. Dileptonic $t\bar{t}$ control regions require the same selections as the $2e$ and 2μ categories with two b tags, but the dilepton invariant mass region around the nominal Z boson mass is vetoed ($50 < m_{\ell\ell} < 70$ GeV or $m_{\ell\ell} > 110$ GeV), and the m_{jj} selection is dropped. Two additional top quark CRs are defined specifically for $t\bar{t}$ events where only one of the two W bosons decays into an electron or a muon, and the lepton is not reconstructed. These events contribute to the $t\bar{t}$ contamination in the 0ℓ categories. The two single-lepton top quark CRs have the same selections as the two W +jets CRs, but in this case the jet and b tag vetoes are inverted to enrich the $t\bar{t}$ composition.

An important feature of the signal is that the two b jets originate from the decay of the h boson, whose mass is known with better precision than that provided by the $b\bar{b}$ invariant mass resolution. The measured jet p_T values are therefore scaled according to their corresponding uncertainty given by the jet energy scale corrections to constrain the dijet invariant mass to $m_{jj} = 125$ GeV. The kinematic constraint on the h boson mass improves the relative four-body invariant mass resolution from 5–6 to 2.5–4.5% for the smallest and largest values of m_A , respectively. Similarly, in the 2ℓ channels, the electron and muon p_T are scaled to a dilepton invariant mass $m_{\ell\ell} = m_Z$. The effect on the m_A resolution of the kinematic constraint on the leptons is much smaller than the one of the jets, because of their better momentum resolution.

In the $2e$ and 2μ categories, the A boson decay chain yields an additional characteristic, which helps distinguish it from SM background. Five helicity-dependent angular observables fully describe the kinematics of the $A \rightarrow Zh \rightarrow \ell\ell b\bar{b}$ decay: the angle between the directions of the Z boson and the beam in the rest frame of the A boson ($\cos\theta^*$); the decay angle between the direction of the negatively charged lepton relative to the Z boson momentum vector in the rest frame of the Z boson ($\cos\theta_1$), which is sensitive to the transverse polarization of the Z boson along its momentum vector; the angle between a jet from the h boson and the h boson momentum vector in the h boson rest frame ($\cos\theta_2$); the angle between the Z and h boson decay planes in the rest frame of the A boson (Φ); the angle between the h boson decay plane and the plane where the h boson and the beam directions lie in the A boson rest frame (Φ_1). The discriminating power and low cross-correlation make these angles suitable as input to a likelihood ratio multivariate discriminator. This angular discriminant is defined as:

$$\mathcal{D}(x_1, \dots, x_N) = \frac{\prod_{i=1}^N s_i(x_i)}{\prod_{i=1}^N s_i(x_i) + \prod_{i=1}^N b_i(x_i)} \quad (1)$$

where the index i runs from 1 to 5 and corresponds to the number N of angular variables x_i , and s_i and b_i are the signal and Z +jets background probability density functions of the i -th variable, respectively. A selection of $\mathcal{D} > 0.5$ is applied in all $2e$ and 2μ SRs and CRs, except those with three b tags due to the low event count. This working point retains 80% of the signal efficiency and rejects 50% of the Z +jets background.

Considering that top quark pair production may be as large as 50% of the total background in certain regions of the parameter space, a second likelihood ratio discriminator is built specifically to reject the $t\bar{t}$ events. This discriminator uses only the $m_{\ell\ell}$ and p_T^{miss} variables. The background probability density function considers only the top quark background in order to achieve the maximum separation between events with a genuine leptonically decaying Z boson recoiling against a pair of jets and the more complex topologies such as $t\bar{t}$ decays. Selecting events with a discriminator output larger than 0.5 rejects 75% of the $t\bar{t}$ events with a signal efficiency of 85%. This selection is applied to the dileptonic SRs and to the Z +jets CRs.

The SRs and CRs selections are summarized in Table 1. The product of the signal acceptance and selection efficiency as a function of m_A is presented in Fig. 2 separately for the gluon–gluon fusion and b quark associated production modes.

6 Systematic uncertainties

The uncertainties in the trigger efficiency and the electron, muon, and τ lepton reconstruction, identification, and isolation efficiencies are evaluated through studies of events with dilepton invariant mass around the Z boson mass, and the variation of the event yields with respect to the expectation from simulation amount to approximately 2–3% for the categories with charged leptons, and 1% in the 0ℓ categories [15, 16, 20]. The impact of the lepton energy and momentum scale and resolution is small after the kinematic constraint on $m_{\ell\ell}$. The jet energy scale and resolution [24] affect both the selection efficiencies and the shape of the p_T^{miss} and $m_{Z_h}^T$ distributions, and are negligible in the 2ℓ channels after the kinematic constraint on the dijet mass has been applied. The jet four-momentum is varied by the corresponding uncertainties, and the effect is propagated to the final distributions. The jet energy scale is responsible for a 2–6% variation in the numbers of background and signal events; the jet energy resolution contributes an additional 1–2% uncertainty. The effects of jet energy scale and resolution

Table 1 Definition of the signal and control regions. In 2ℓ regions, the leptons are required to have opposite electric charge. The entries marked with † indicate that the p_T^{miss} is calculated subtracting the four momentum of the lepton

Region	0ℓ SR	0ℓ Z CR	1ℓ W CR	1ℓ t CR	2ℓ SR	2ℓ Z CR	2ℓ t CR
Leptons	e, μ , τ veto		1e or 1 μ		2e or 2 μ		
p_T^ℓ (GeV)	-		> 55		> 55, 20		
$m_{\ell\ell}$ (GeV)	-	-	-	-	70 < $m_{\ell\ell}$ < 110		< 70, > 110
p_T^{miss} (GeV)	> 200	> 200	> 200†	> 200†	< 100	< 100	-
Jets	≥ 2 or 3	≥ 2	≤ 3	≥ 4	≥ 2 or 3	≥ 2	≥ 2
b-tagged jets	1, 2, or 3	0, 1, 2, or 3	0	≥ 1	1, 2, or 3	0, 1, 2, or 3	≥ 2
p_T^{bb} (GeV)	> 200	> 200	> 200	> 200	-	-	-
m_{jj} (GeV)	> 100, < 140	< 100, > 140	-	-	> 100, < 140	< 100, > 140	-
$\Delta\phi(j, \vec{p}_T^{\text{miss}})$	< 0.4	< 0.4	-	-	-	-	-
Angular \mathcal{D}	-	-	-	-	> 0.5	> 0.5	-
Top quark \mathcal{D}	-	-	-	-	> 0.5	> 0.5	-

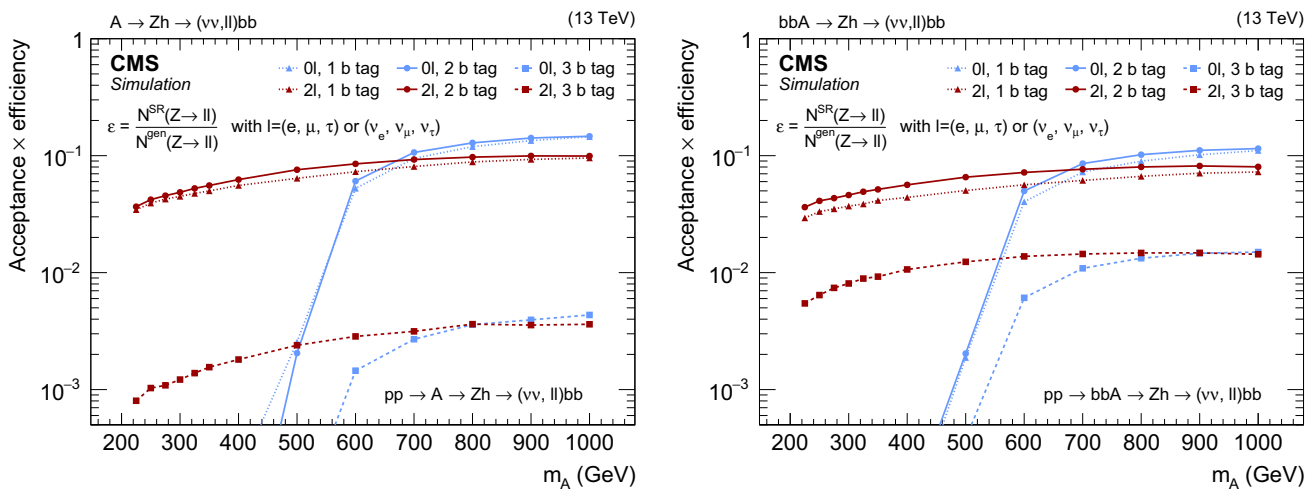


Fig. 2 Product of the signal acceptance and selection efficiency ϵ for an A boson produced via gluon–gluon fusion (left) and in association with b quarks (right) as a function of m_A . The number of events passing

the signal region selections is denoted as N^{SR} , and N^{gen} is the number of events generated before applying any selection

uncertainties, as well as the energy variation of the unclustered objects in the event, are propagated to the p_T^{miss} and $m_{Z\text{h}}^{\text{T}}$ distributions. The b tagging uncertainty [25] in the signal yield depends on the jet p_T and thus on the mass of the resonance, and the impact on the event yield ranges from 2 to 4% in the 1 b tag category, 4 to 8% in the 2 b tag category, and 8 to 12% in the 3 b tag category.

The signal and background event yields are affected by the uncertainties on the choice of PDFs [46] and the factorization and renormalization scale uncertainties. The former are derived with SYSCALC [47], and the latter are estimated by varying the corresponding scales up and down by a factor of two [48]. The effect of both these uncertainties can be as large as 30% depending on the generated signal mass. The effect of the PDF uncertainties on the signal and background lepton acceptance is estimated to be an average of 3%

per lepton. The top quark background is also affected by the uncertainty associated with the simulated p_T spectrum of top quarks [38], which results in up to a 14% yield uncertainty. The V+jets backgrounds are affected by the uncertainties on the QCD and EW NLO corrections, as described in Sect. 4.

A systematic uncertainty is assigned to the interpolation between the two mass sidebands to the SR, defined as the difference in the ratio between data and simulated background in the lower and upper sidebands, and ranges between 2 and 10% depending on the channel. The extrapolation to the 3 b tag regions is covered by a large uncertainty (20–46%) assigned to the overall background normalization, and derived by taking the ratio between data and the simulation in the 3 b tag control regions. In the dilepton categories, a dedicated uncertainty is introduced to cover for minor mis-modeling effects. The background distribution is reweighted

Table 2 Summary of statistical and systematic uncertainties for backgrounds and signal. The uncertainties marked with \checkmark are also propagated to the m_{Z_h} and $m_{Z_h}^T$ distributions

	Shape	Main backgrounds (V+jets, tt)	Other backgrounds (t+X, VV, Vh)	Signal
Lepton and trigger efficiency	\checkmark	–	2–3%	2–3%
Jet energy scale	\checkmark	–	5%	2–6%
Jet energy resolution	\checkmark	–	2%	1–2%
b tagging	\checkmark	–	4%	4–12%
Unclustered p_T^{miss}	\checkmark	–	1%	1%
Pileup	\checkmark	–	1%	1%
PDF	\checkmark	–	3–5%	4–8%
Top quark p_T modeling	\checkmark	8–14% (only $t\bar{t}$)	–	–
Fact. and renorm. scale	\checkmark	–	2–6%	6–14%
Monte Carlo modeling	\checkmark		1–15 %	–
Monte Carlo event count	\checkmark		1–20%	–
Interpolation to SR			2–10%	–
Extrapolation to ≥ 3 b tag SR		20–46% (≥ 3 b tag only)		–
Cross section		–	2–10%	–
Integrated luminosity		–	2.5%	2.5%

Table 3 Scale factors for the main backgrounds, as derived by the combined fit in the background-only hypothesis, with respect to the event yield from simulated samples

Background	Scale factor
Z+jets	0.993 ± 0.018
Z+b	1.214 ± 0.021
Z+b \bar{b}	1.007 ± 0.025
t \bar{t}	0.996 ± 0.014
W+jets	0.980 ± 0.023

with a linear function of the event centrality (defined as the ratio between the sums of the p_T and the energy of the two leptons and two jets in the rest frame of the four objects) in all simulated events, and the effect is propagated to the m_{Z_h} distributions as a systematic uncertainty.

Additional systematic uncertainties affect the event yields of backgrounds and signal come from pileup contributions and integrated luminosity [49]. The uncertainty from the limited number of simulated events is treated as in Ref. [50]. A summary of the systematic uncertainties is reported in Table 2.

7 Results and interpretation

The signal search is carried out by performing a combined signal and background maximum likelihood fit to the number of events in the CRs, and the binned m_{Z_h} or $m_{Z_h}^T$ distributions in the SRs. Systematic uncertainties are treated as nuisance parameters and are profiled in the statistical inter-

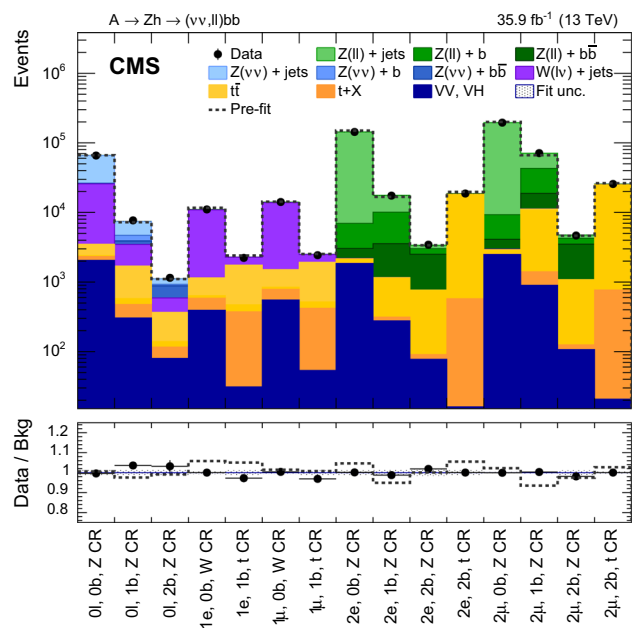


Fig. 3 Pre- (dashed gray lines) and post-fit (stacked histograms) numbers of events in the different control regions used in the fit. The label in each bin summarizes the control region definition, the selection on the number and flavor of the leptons, and the number of b-tagged jets. The bottom panel depicts the ratio between the data and the SM backgrounds

pretation [51–53]. The asymptotic approximation [54] of the modified frequentist CL_s criterion [51, 52] is used to determine limits on the signal cross section at 95% confidence level (CL). The background-only hypothesis is tested against the combined signal+background hypothesis in the nine cate-

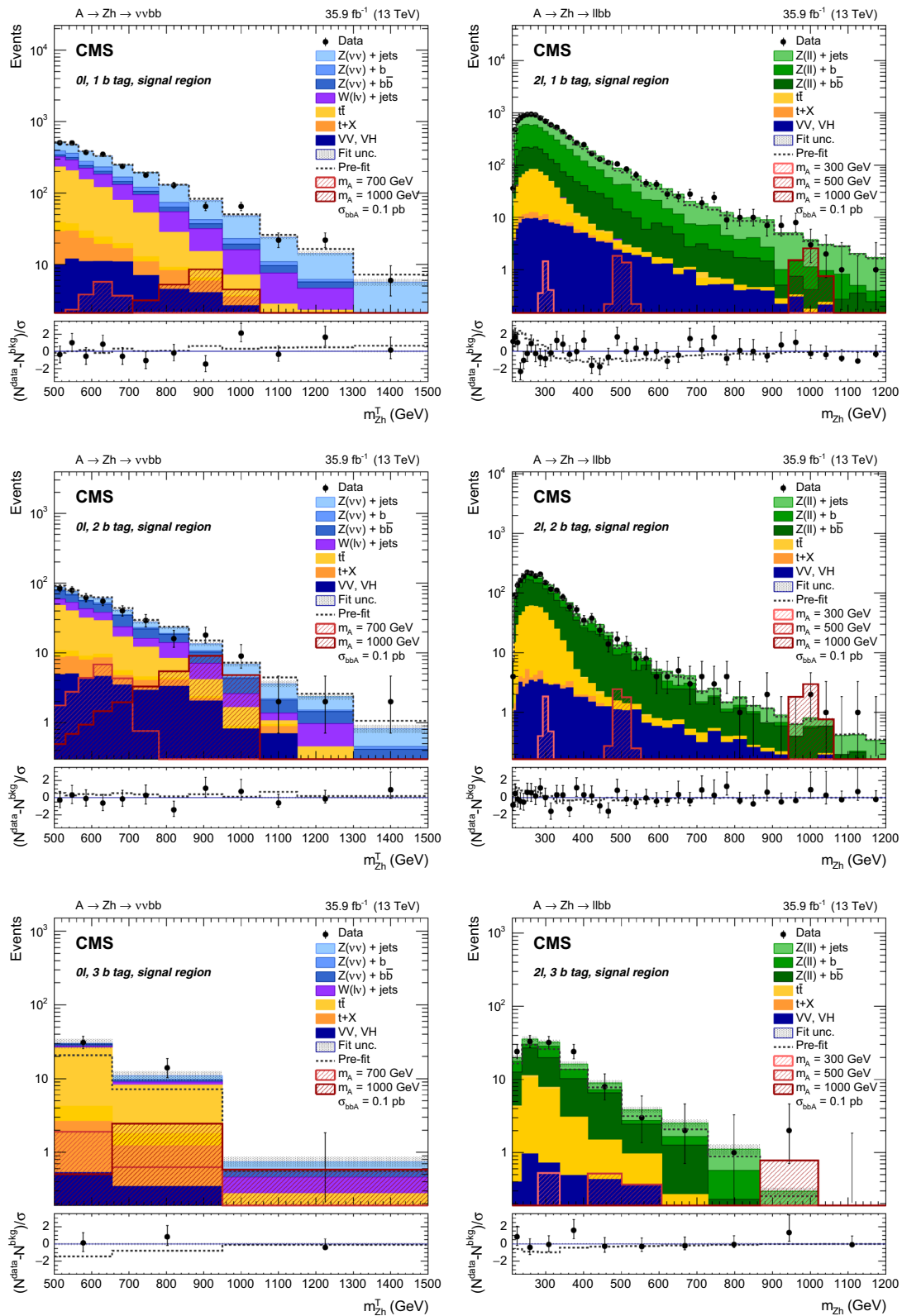


Fig. 4 Distributions of the $m_{Z_h}^T$ variable in the 0ℓ categories (left) and m_{Z_h} in the 2ℓ categories (right), in the 1 b tag (upper), 2 b tag (center), and 3 b tag (lower) SRs. In the 2ℓ categories, the contribution of the $2e$ and 2μ channels have been summed. The gray dotted line represents the sum of the background before the fit; the shaded area

represents the post-fit uncertainty. The hatched red histograms represent signals produced in association with b quarks and corresponding to $\sigma_A \mathcal{B}(A \rightarrow Zh) \mathcal{B}(h \rightarrow b\bar{b}) = 0.1 \text{ pb}$. The bottom panels depict the pulls in each bin, $(N^{\text{data}} - N^{\text{bkg}})/\sigma$, where σ is the statistical uncertainty in data

Table 4 Expected and observed event yields after the fit in the signal regions. The dielectron and dimuon categories are summed together. The “–” symbol represents backgrounds with no simulated events passing the selections. The signal yields refer to pre-fit values correspond-

ing to a cross section multiplied by $\mathcal{B}(A \rightarrow Zh) \mathcal{B}(h \rightarrow b\bar{b})$ of 0.1 pb (gluon–gluon fusion for $m_A = 300$ GeV, and in association with b quarks for $m_A = 1000$ GeV)

Signal region	0 ℓ , 1 b tag	0 ℓ , 2 b tag	0 ℓ , ≥ 3 b tag	2 ℓ , 1 b tag	2 ℓ , 2 b tag	2 ℓ , ≥ 3 b tag
Data	2452 \pm 50	398 \pm 20	45 \pm 7	10,512 \pm 103	2188 \pm 47	129 \pm 11
Z+jets	740 \pm 12	48 \pm 1	2.0 \pm 0.2	4118 \pm 15	175 \pm 1	18 \pm 1
Z+b	220 \pm 6	13 \pm 1	0.46 \pm 0.06	4127 \pm 18	365 \pm 3	23 \pm 1
Z+b \bar{b}	134 \pm 3	86 \pm 2	2.5 \pm 0.3	1547 \pm 11	1113 \pm 7	51 \pm 2
t+X	74 \pm 3	18 \pm 1	3.0 \pm 0.4	25 \pm 0	10.0 \pm 0.1	–
t \bar{t}	750 \pm 12	143 \pm 3	31 \pm 3	592 \pm 3	473 \pm 3	26 \pm 1
VV, Vh	76 \pm 2	32 \pm 1	0.93 \pm 0.11	139 \pm 1	53 \pm 1	3.5 \pm 0.1
W+jets	458 \pm 13	65 \pm 3	2.4 \pm 0.3	3.7 \pm 0.1	–	–
Total bkg.	2451 \pm 26	405 \pm 8	42 \pm 5	10,552 \pm 35	2189 \pm 12	121 \pm 3
Pre-fit bkg.	2467 \pm 26	427 \pm 8	28 \pm 5	10,740 \pm 35	2250 \pm 12	100 \pm 3
$m_A = 300$ GeV	–	–	–	3.1 \pm 0.2	3.3 \pm 0.2	0.10 \pm 0.01
$m_A = 1000$ GeV	27.3 \pm 5.2	28.6 \pm 5.4	3.5 \pm 0.7	5.4 \pm 1.0	6.1 \pm 1.2	1.2 \pm 0.2

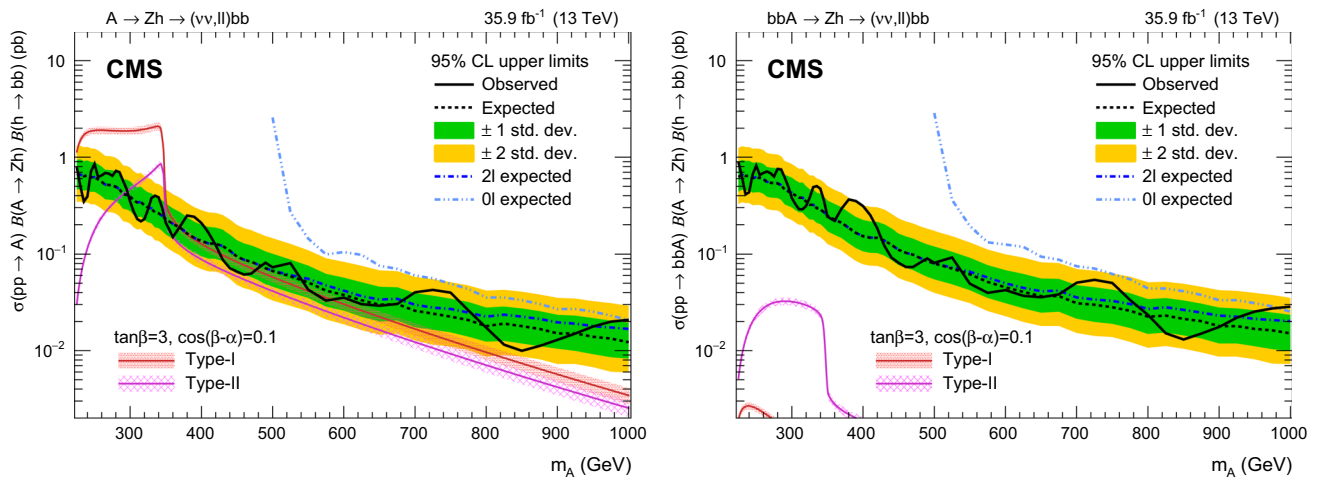


Fig. 5 Observed (solid black) and expected (dotted black) 95% CL upper limits on $\sigma_A \mathcal{B}(A \rightarrow Zh) \mathcal{B}(h \rightarrow b\bar{b})$ for an A boson produced via gluon–gluon fusion (left) and in association with b quarks (right) as a function of m_A . The blue dashed lines represent the expected limits of the 0 ℓ and 2 ℓ categories separately. The red and magenta solid curves

and their shaded areas correspond to the product of the cross sections and the branching fractions and the relative uncertainties predicted by the 2HDM Type-I and Type-II for the arbitrary parameters $\tan \beta = 3$ and $\cos(\beta - \alpha) = 0.1$

gies, split according to the number and flavor of the leptons and number of b-tagged jets. The normalizations of the main backgrounds (Z+jets, Z+b, Z+b \bar{b} , t \bar{t} , W+jets) are allowed to float in the fit, and are constrained in the CRs. The multiplicative scale factors for the main backgrounds determined by the fit are reported in Table 3, and the overall event yields in the CRs are shown in Fig. 3 before and after the fit. The expected and observed number of events in the SRs are reported in Table 4, and the m_{Zh} and m_{Zh}^T distributions are shown in Fig. 4.

The data are well described by the SM processes. Upper limits are derived on the product of the cross section for a heavy pseudoscalar boson A and the branching fractions for

the decays $A \rightarrow Zh$ and $h \rightarrow b\bar{b}$. The limits are obtained by considering the A boson produced via the gluon–gluon fusion and b quark associated production processes separately, in the approximation where the natural width of the A boson Γ_A is smaller than the experimental resolution, and are reported in Fig. 5. An upper limit at 95% CL on the number of signal events is set on $\sigma_A \mathcal{B}(A \rightarrow Zh) \mathcal{B}(h \rightarrow b\bar{b})$, excluding above 1 pb for m_A near the kinematic threshold, ≈ 0.3 pb for $m_A \approx 2m_t$, and as low as 0.02 pb at the high end (1000 GeV) of the considered mass range. The sensitivity of the analysis is limited by the amount of data, and not by systematic uncertainties. These results extend the search for a 2HDM pseudoscalar boson A for mass up to 1 TeV, which

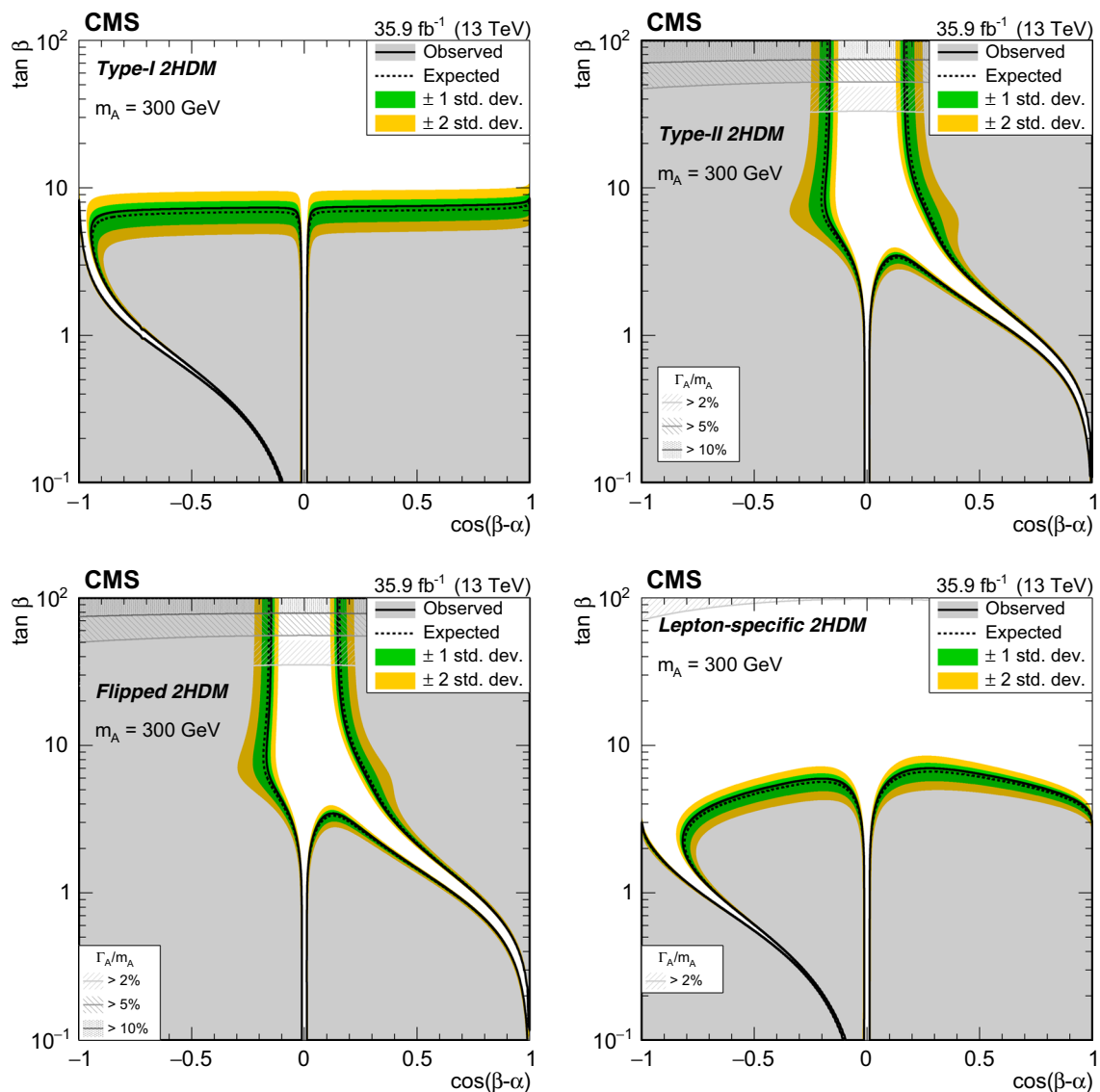


Fig. 6 Observed and expected (with ± 1 , ± 2 standard deviation bands) exclusion limits for Type-I (upper left), Type-II (upper right), flipped (lower left), lepton-specific (lower right) models, as a function of $\cos(\beta - \alpha)$ and $\tan \beta$. Contours are derived from the projection on the 2HDM parameter space for the $m_A = 300$ GeV signal hypothesis.

is a kinematic region previously unexplored by CMS in the 8 TeV data analysis [10]. When m_A is larger than 1 TeV, the CMS analysis with merged jets [11] retains a better sensitivity. The sensitivity is comparable to the ATLAS search [12], which observed a mild local (global) excess of 3.6 (2.4) standard deviations corresponding to $m_A \approx 440$ GeV in final states with 2μ and 3 or more b-tagged jets. A slight deficit is observed by CMS in the corresponding region.

The results are interpreted in terms of Type-I, Type-II, “lepton-specific”, and “flipped” 2HDM formulations [5]. In the scenario with $\cos(\beta - \alpha) = 0.1$ and $\tan \beta = 3$, an A boson up to 380 and 350 GeV is excluded in 2HDM Type-I and

Type-II, respectively, as depicted in Fig. 5. These exclusion limits are used to constrain the two-dimensional plane of the 2HDM parameters $[\cos(\beta - \alpha), \tan \beta]$ as reported in Fig. 6, with fixed $m_A = 300$ GeV in the range $0.1 \leq \tan \beta \leq 100$ and $-1 \leq \cos(\beta - \alpha) \leq 1$, using the convention $0 < \beta - \alpha < \pi$. Because of the suppressed A boson cross section and $\mathcal{B}(A \rightarrow Z\gamma)$, the region near $\cos(\beta - \alpha) \approx 0$ is not accessible in this search. On the other hand, $\mathcal{B}(h \rightarrow b\bar{b})$ vanishes in the diagonal regions corresponding to α close to 0 in Type-II and flipped 2HDM, and $\alpha \rightarrow \pm\pi/2$ in Type-I and lepton-specific scenarios. The exclusion as a function of m_A , fixing $\cos(\beta - \alpha) = 0.1$, is also reported in Fig. 7.

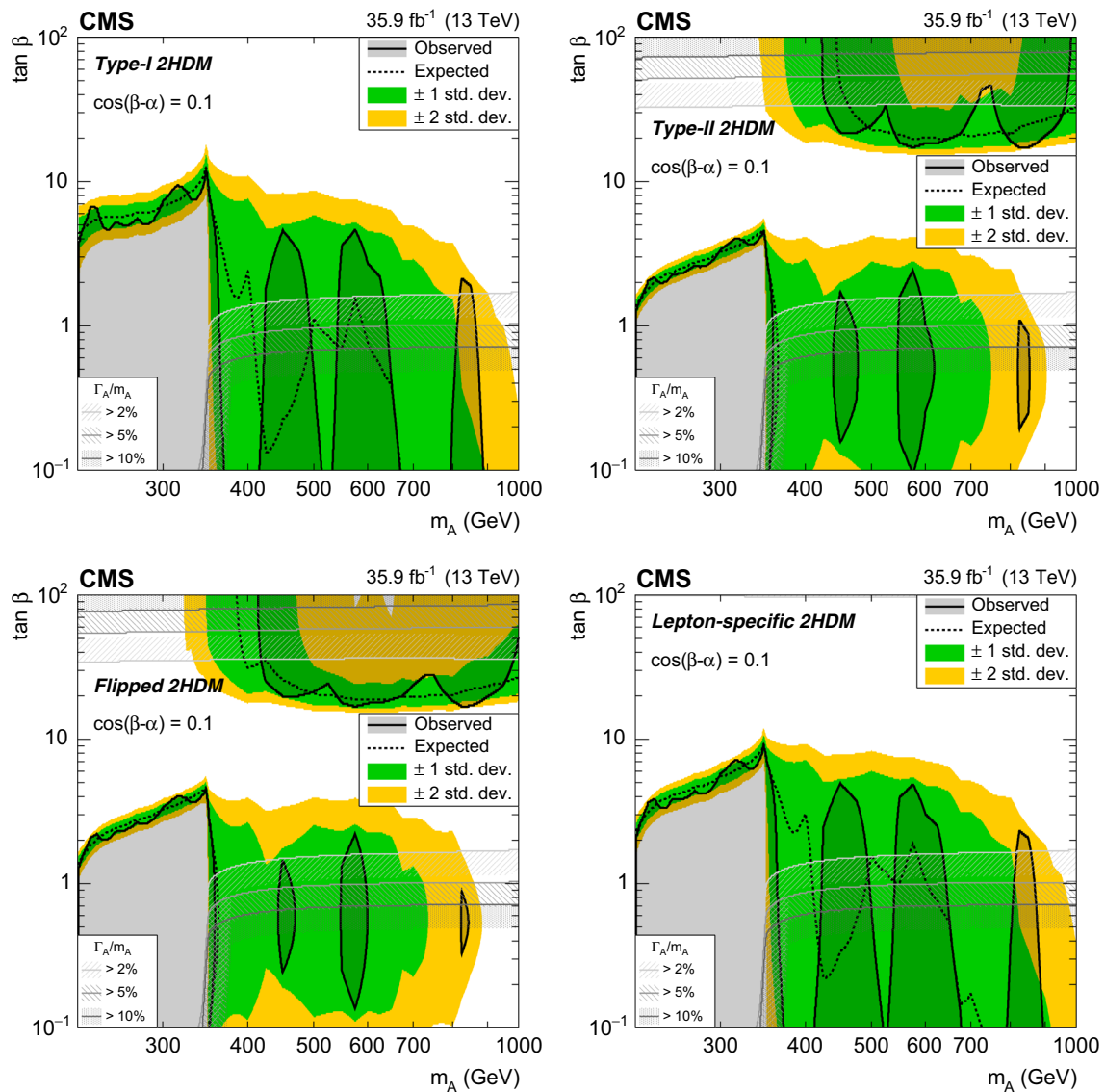


Fig. 7 Observed and expected (with ± 1 , ± 2 standard deviation bands) exclusion limits for Type-I (upper left), Type-II (upper right), flipped (lower left), lepton-specific (lower right) models, as a function of m_A and $\tan \beta$, fixing $\cos(\beta - \alpha) = 0.1$. The excluded region is represented

by the shaded gray area. The regions of the parameter space where the natural width of the A boson Γ_A is comparable to the experimental resolution and thus the narrow width approximation is not valid are represented by the hatched gray areas

8 Summary

A search is presented in the context of an extended Higgs boson sector for a heavy pseudoscalar boson A that decays into a Z boson and an h boson with mass of 125 GeV, with the Z boson decaying into electrons, muons, or neutrinos, and the h boson into $b\bar{b}$. The SM backgrounds are suppressed by using the characteristics of the considered signal, namely the production and decay angles of the A, Z, and h bosons, and by improving the A mass resolution through a kinematic constraint on the reconstructed invariant mass of the h boson candidate. No excess of data over the background prediction is observed. Upper limits are set at 95% confi-

dence level on the product of the A boson cross sections and the branching fractions $\sigma_A \mathcal{B}(A \rightarrow Zh) \mathcal{B}(h \rightarrow b\bar{b})$, which exclude 1 to 0.01 pb in the 225–1000 GeV mass range, and are comparable to the corresponding ATLAS search. Interpretations are given in the context of Type-I, Type-II, flipped, and lepton-specific two-Higgs-doublet model formulations, thereby reducing the allowed parameter space for extensions of the SM with respect to previous CMS searches.

Acknowledgements We congratulate our colleagues in the CERN accelerator departments for the excellent performance of the LHC and thank the technical and administrative staffs at CERN and at other CMS institutes for their contributions to the success of the CMS effort. In addition, we gratefully acknowledge the computing centers and personnel of the Worldwide LHC Computing Grid for delivering so effec-

tively the computing infrastructure essential to our analyses. Finally, we acknowledge the enduring support for the construction and operation of the LHC and the CMS detector provided by the following funding agencies: BMFWF and FWF (Austria); FNRS and FWO (Belgium); CNPq, CAPES, FAPERJ, and FAPESP (Brazil); MES (Bulgaria); CERN; CAS, MoST, and NSFC (China); COLCIENCIAS (Colombia); MSES and CSF (Croatia); RPF (Cyprus); SENESCYT (Ecuador); MoER, ERC IUT, and ERDF (Estonia); Academy of Finland, MEC, and HIP (Finland); CEA and CNRS/IN2P3 (France); BMBF, DFG, and HGF (Germany); GSRT (Greece); NKFI (Hungary); DAE and DST (India); IPM (Iran); SFI (Ireland); INFN (Italy); MSIP and NRF (Republic of Korea); LAS (Lithuania); MOE and UM (Malaysia); BUAP, CINVESTAV, CONACYT, LNS, SEP, and UASLP-FAI (Mexico); MBIE (New Zealand); PAEC (Pakistan); MSHE and NSC (Poland); FCT (Portugal); JINR (Dubna); MON, RosAtom, RAS and RFBR (Russia); MESTD (Serbia); SEIDI, CPAN, PCTI and FEDER (Spain); Swiss Funding Agencies (Switzerland); MST (Taipei); ThEPCenter, IPST, STAR, and NSTDA (Thailand); TUBITAK and TAEK (Turkey); NASU and SFFR (Ukraine); STFC (United Kingdom); DOE and NSF (USA). Individuals have received support from the Marie-Curie program and the European Research Council and Horizon 2020 Grant, contract No. 675440 (European Union); the Leventis Foundation; the A.P. Sloan Foundation; the Alexander von Humboldt Foundation; the Belgian Federal Science Policy Office; the Fonds pour la Formation à la Recherche dans l'Industrie et dans l'Agriculture (FRIA-Belgium); the Agentschap voor Innovatie door Wetenschap en Technologie (IWT-Belgium); the F.R.S.-FNRS and FWO (Belgium) under the "Excellence of Science – EOS" – be.h project n. 30820817; the Ministry of Education, Youth and Sports (MEYS) of the Czech Republic; the Lendület ("Momentum") Program and the János Bolyai Research Scholarship of the Hungarian Academy of Sciences, the New National Excellence Program ÚNKP, the NKFI research Grants 123842, 123959, 124845, 124850, and 125105 (Hungary); the Council of Science and Industrial Research, India; the HOMING PLUS program of the Foundation for Polish Science, cofinanced from European Union, Regional Development Fund, the Mobility Plus program of the Ministry of Science and Higher Education, the National Science Center (Poland), contracts Harmonia 2014/14/M/ST2/00428, Opus 2014/13/B/ST2/02543, 2014/15/B/ST2/03998, and 2015/19/B/ST2/02861, Sonata-bis 2012/07/E/ST2/01406; the National Priorities Research Program by Qatar National Research Fund; the Programa Estatal de Fomento de la Investigación Científica y Técnica de Excelencia María de Maeztu, Grant MDM-2015-0509 and the Programa Severo Ochoa del Principado de Asturias; the Thalis and Aristeia programs cofinanced by EU-ESF and the Greek NSRF; the Rachadapisek Sompot Fund for Postdoctoral Fellowship, Chulalongkorn University and the Chulalongkorn Academic into Its 2nd Century Project Advancement Project (Thailand); the Welch Foundation, contract C-1845; and the Weston Havens Foundation (USA).

Data Availability Statement This manuscript has no associated data or the data will not be deposited. [Authors' comment: Release and preservation of data used by the CMS Collaboration as the basis for publications is guided by the CMS policy as written in its document "CMS data preservation, re-use and open access policy" (<https://cms-docdb.cern.ch/cgi-bin/PublicDocDB/RetrieveFile?docid=6032&filename=CMSDataPolicyV1.2.pdf&version=2>).]

Open Access This article is distributed under the terms of the Creative Commons Attribution 4.0 International License (<http://creativecommons.org/licenses/by/4.0/>), which permits unrestricted use, distribution, and reproduction in any medium, provided you give appropriate credit to the original author(s) and the source, provide a link to the Creative Commons license, and indicate if changes were made. Funded by SCOAP³.

References

1. ATLAS Collaboration, Observation of a new particle in the search for the Standard Model Higgs boson with the ATLAS detector at the LHC. *Phys. Lett. B* **716**, 1 (2012). <https://doi.org/10.1016/j.physletb.2012.08.020>. arXiv:1207.7214
2. CMS Collaboration, Observation of a new boson at a mass of 125 GeV with the CMS experiment at the LHC. *Phys. Lett. B* **716**, 30 (2012). <https://doi.org/10.1016/j.physletb.2012.08.021>. arXiv:1207.7235
3. ATLAS and CMS Collaborations, Combined measurement of the Higgs boson mass in pp collisions at $\sqrt{s} = 7$ and 8 TeV with the ATLAS and CMS experiments. *Phys. Rev. Lett.* **114**, 191803 (2015). <https://doi.org/10.1103/PhysRevLett.114.191803>. arXiv:1503.07589
4. ATLAS and CMS Collaborations, Measurements of the Higgs boson production and decay rates and constraints on its couplings from a combined ATLAS and CMS analysis of the LHC pp collision data at $\sqrt{s} = 7$ and 8 TeV. *JHEP* **08**, 045 (2016). [https://doi.org/10.1007/JHEP08\(2016\)045](https://doi.org/10.1007/JHEP08(2016)045). arXiv:1606.02266
5. G.C. Branco et al., Theory and phenomenology of two-Higgs-doublet models. *Phys. Rept.* **516**, 1 (2012). <https://doi.org/10.1016/j.physrep.2012.02.002>. arXiv:1106.0034
6. S.P. Martin, A Supersymmetry primer. *Adv. Ser. Direct. HEP* **21**, 1 (2010). https://doi.org/10.1142/9789814307505_0001. arXiv:hep-ph/9709356
7. J.E. Kim, Light pseudoscalars, particle physics and cosmology. *Phys. Rept.* **150**, 1 (1987). [https://doi.org/10.1016/0370-1573\(87\)90017-2](https://doi.org/10.1016/0370-1573(87)90017-2)
8. L. Fromme, S.J. Huber, M. Seniuch, Baryogenesis in the two-Higgs doublet model. *JHEP* **11**, 038 (2006). <https://doi.org/10.1088/1126-6708/2006/11/038>. arXiv:hep-ph/0605242
9. CMS Collaboration, Combined measurements of Higgs boson couplings in proton–proton collisions at $\sqrt{s} = 13$ TeV (2018). arXiv:1809.10733 (Submitted to EPJC)
10. CMS Collaboration, Search for a pseudoscalar boson decaying into a Z boson and the 125 GeV Higgs boson in $\ell^+ \ell^- b \bar{b}$ final states. *Phys. Lett. B* **748**, 221 (2015). <https://doi.org/10.1016/j.physletb.2015.07.010>. arXiv:1504.04710
11. CMS Collaboration, Search for heavy resonances decaying into a vector boson and a Higgs boson in final states with charged leptons, neutrinos and b quarks at $\sqrt{s} = 13$ TeV. *JHEP* **11**, 172 (2018). [https://doi.org/10.1007/JHEP11\(2018\)172](https://doi.org/10.1007/JHEP11(2018)172). arXiv:1807.02826
12. ATLAS Collaboration, Search for heavy resonances decaying into a W or Z boson and a Higgs boson in final states with leptons and b-jets in 36 fb⁻¹ of $\sqrt{s} = 13$ TeV pp collisions with the ATLAS detector. *JHEP* **03** (2018) 174. [https://doi.org/10.1007/JHEP03\(2018\)174](https://doi.org/10.1007/JHEP03(2018)174). arXiv:1712.06518
13. CMS Collaboration, The CMS experiment at the CERN LHC. *JINST* **3**, S08004 (2008). <https://doi.org/10.1088/1748-0221/3/08/S08004>
14. CMS Collaboration, Description and performance of track and primary-vertex reconstruction with the CMS tracker. *JINST* **9**, P10009 (2014). <https://doi.org/10.1088/1748-0221/9/10/P10009>. arXiv:1405.6569
15. CMS Collaboration, Performance of electron reconstruction and selection with the CMS detector in proton-proton collisions at $\sqrt{s} = 8$ TeV. *JINST* **10**, P06005 (2015). <https://doi.org/10.1088/1748-0221/10/06/P06005>. arXiv:1502.02701
16. CMS Collaboration, Performance of CMS muon reconstruction in pp collision events at $\sqrt{s} = 7$ TeV. *JINST* **7**, P10002 (2012). <https://doi.org/10.1088/1748-0221/7/10/P10002>. arXiv:1206.4071
17. CMS Collaboration, The CMS trigger system. *JINST* **12**, P01020 (2017). <https://doi.org/10.1088/1748-0221/12/01/P01020>. arXiv:1609.02366

18. CMS Collaboration, Particle-flow reconstruction and global event description with the CMS detector. *JINST* **12**, P10003 (2017). <https://doi.org/10.1088/1748-0221/12/10/P10003>. arXiv:1706.04965
19. CMS Collaboration, Pileup removal algorithms. CMS Physics Analysis Summary CMS-PAS-JME-14-001, CERN (2014)
20. CMS Collaboration, Reconstruction and identification of τ lepton decays to hadrons and ν_τ at CMS. *JINST* **11**, P01019 (2016). <https://doi.org/10.1088/1748-0221/11/01/P01019>. arXiv:1510.07488
21. M. Cacciari, G.P. Salam, G. Soyez, The anti- k_t jet clustering algorithm. *JHEP* **04**, 063 (2008). <https://doi.org/10.1088/1126-6708/2008/04/063>. arXiv:0802.1189
22. M. Cacciari, G.P. Salam, G. Soyez, FastJet user manual. *Eur. Phys. J. C* **72**, 1896 (2012). <https://doi.org/10.1140/epjc/s10052-012-1896-2>. arXiv:1111.6097
23. M. Cacciari, G.P. Salam, G. Soyez, The catchment area of jets. *JHEP* **04**, 005 (2008). <https://doi.org/10.1088/1126-6708/2008/04/005>. arXiv:0802.1188
24. CMS Collaboration, Jet energy scale and resolution in the CMS experiment in pp collisions at 8 TeV. *JINST* **12**, P02014 (2017). <https://doi.org/10.1088/1748-0221/12/02/P02014>. arXiv:1607.03663
25. CMS Collaboration, Identification of heavy-flavour jets with the CMS detector in pp collisions at 13 TeV. *JINST* **13**, P05011 (2018). <https://doi.org/10.1088/1748-0221/13/05/P05011>. arXiv:1712.07158
26. J. Alwall et al., The automated computation of tree-level and next-to-leading order differential cross sections, and their matching to parton shower simulations. *JHEP* **07**, 079 (2014). [https://doi.org/10.1007/JHEP07\(2014\)079](https://doi.org/10.1007/JHEP07(2014)079). arXiv:1405.0301
27. P. Artoisenet, R. Frederix, O. Mattelaer, R. Rietkerk, Automatic spin-entangled decays of heavy resonances in Monte Carlo simulations. *JHEP* **03**, 015 (2013). [https://doi.org/10.1007/JHEP03\(2013\)015](https://doi.org/10.1007/JHEP03(2013)015). arXiv:1212.3460
28. D. Eriksson, J. Rathsman, O. Stål, 2HDMC – two-Higgs-doublet model calculator physics and manual. *Comput. Phys. Commun.* **181**, 189 (2010). <https://doi.org/10.1016/j.cpc.2009.09.011>. arXiv:0902.0851
29. R.V. Harlander, S. Liebler, H. Mantler, SusHi: a program for the calculation of Higgs production in gluon fusion and bottom-quark annihilation in the Standard Model and the MSSM. *Comput. Phys. Commun.* **184**, 1605 (2013). <https://doi.org/10.1016/j.cpc.2013.02.006>. arXiv:1212.3249
30. Particle Data Group Collaboration, Review of particle physics. *Phys. Rev. D* **98**, 030001 (2018). <https://doi.org/10.1103/PhysRevD.98.030001>
31. J. Alwall et al., Comparative study of various algorithms for the merging of parton showers and matrix elements in hadronic collisions. *Eur. Phys. J. C* **53**, 473 (2008). <https://doi.org/10.1140/epjc/s10052-007-0490-5>. arXiv:0706.2569
32. Y. Li, F. Petriello, Combining QCD and electroweak corrections to dilepton production in FEWZ. *Phys. Rev. D* **86**, 094034 (2012). <https://doi.org/10.1103/PhysRevD.86.094034>. arXiv:1208.5967
33. S. Kallweit et al., NLO QCD+EW predictions for V+jets including off-shell vector-boson decays and multijet merging. *JHEP* **04**, 021 (2016). [https://doi.org/10.1007/JHEP04\(2016\)021](https://doi.org/10.1007/JHEP04(2016)021). arXiv:1511.08692
34. P. Nason, A new method for combining NLO QCD with shower Monte Carlo algorithms. *JHEP* **11**, 040 (2004). <https://doi.org/10.1088/1126-6708/2004/11/040>. arXiv:hep-ph/0409146
35. S. Frixione, P. Nason, C. Oleari, Matching NLO QCD computations with parton shower simulations: the POWHEG method. *JHEP* **11**, 070 (2007). <https://doi.org/10.1088/1126-6708/2007/11/070>. arXiv:0709.2092
36. S. Alioli, P. Nason, C. Oleari, E. Re, A general framework for implementing NLO calculations in shower Monte Carlo programs: the POWHEG BOX. *JHEP* **06**, 043 (2010). [https://doi.org/10.1007/JHEP06\(2010\)043](https://doi.org/10.1007/JHEP06(2010)043). arXiv:1002.2581
37. M. Czakon, A. Mitov, Top++: a program for the calculation of the top-pair cross-section at hadron colliders. *Comput. Phys. Commun.* **185**, 2930 (2014). <https://doi.org/10.1016/j.cpc.2014.06.021>. arXiv:1112.5675
38. CMS Collaboration, Measurement of differential cross sections for top quark pair production using the lepton+jets final state in proton-proton collisions at 13 TeV. *Phys. Rev. D* **95**, 092001 (2017). <https://doi.org/10.1103/PhysRevD.95.092001>. arXiv:1610.04191
39. R. Frederix, S. Frixione, Merging meets matching in MC@NLO. *JHEP* **12**, 061 (2012). [https://doi.org/10.1007/JHEP12\(2012\)061](https://doi.org/10.1007/JHEP12(2012)061). arXiv:1209.6215
40. NNPDF Collaboration, Parton distributions for the LHC Run II. *JHEP* **04**, 040 (2015). [https://doi.org/10.1007/JHEP04\(2015\)040](https://doi.org/10.1007/JHEP04(2015)040). arXiv:1410.8849
41. T. Sjöstrand, S. Mrenna, P. Skands, A brief introduction to PYTHIA 8.1. *Comput. Phys. Commun.* **178**, 852 (2008). <https://doi.org/10.1016/j.cpc.2008.01.036>. arXiv:0710.3820
42. T. Sjöstrand, S. Mrenna, P. Skands, PYTHIA 6.4 physics and manual. *JHEP* **05**, 026 (2006). <https://doi.org/10.1088/1126-6708/2006/05/026>. arXiv:hep-ph/0603175
43. CMS Collaboration, Event generator tunes obtained from underlying event and multiparton scattering measurements. *Eur. Phys. J. C* **76**, 155 (2016). <https://doi.org/10.1140/epjc/s10052-016-3988-x>. arXiv:1512.00815
44. CMS Collaboration, Investigations of the impact of the parton shower tuning in Pythia 8 in the modelling of tt at $\sqrt{s} = 8$ and 13 TeV. CMS Physics Analysis Summary CMS-PAS-TOP-16-021, CERN (2016)
45. GEANT4 Collaboration, GEANT4—a simulation toolkit. *Nucl. Instrum. Meth. A* **506**, 250 (2003). [https://doi.org/10.1016/S0168-9002\(03\)01368-8](https://doi.org/10.1016/S0168-9002(03)01368-8)
46. J. Butterworth et al., PDF4LHC recommendations for LHC Run II. *J. Phys. G* **43**, 23001 (2016). <https://doi.org/10.1088/0954-3899/43/2/023001>. arXiv:1510.03865
47. A. Kalogeropoulos, J. Alwall, The SysCalc code: a tool to derive theoretical systematic uncertainties (2018). arXiv:1801.08401
48. S. Catani, D. de Florian, M. Grazzini, P. Nason, Soft gluon resummation for Higgs boson production at hadron colliders. *JHEP* **07**, 028 (2003). <https://doi.org/10.1088/1126-6708/2003/07/028>. arXiv:hep-ph/0306211
49. CMS Collaboration, CMS luminosity measurement for the 2016 data taking period. CMS Physics Analysis Summary CMS-PAS-LUM-17-001, CERN (2017)
50. R. Barlow, C. Beeston, Fitting using finite Monte Carlo samples. *Comput. Phys. Commun.* **77**, 219 (1993). [https://doi.org/10.1016/0010-4655\(93\)90005-W](https://doi.org/10.1016/0010-4655(93)90005-W)
51. T. Junk, Confidence level computation for combining searches with small statistics. *Nucl. Instrum. Meth. A* **434**, 435 (1999). [https://doi.org/10.1016/S0168-9002\(99\)00498-2](https://doi.org/10.1016/S0168-9002(99)00498-2). arXiv:hep-ex/9902006
52. A.L. Read, Presentation of search results: the CL_s technique. *J. Phys. G* **28**, 2693 (2002). <https://doi.org/10.1088/0954-3899/28/10/313>
53. ATLAS and CMS Collaborations, Procedure for the LHC Higgs boson search combination in Summer 2011. CMS Note CMS-NOTE-2011-005, ATL-PHYS-PUB-2011-11, CERN (2011)
54. G. Cowan, K. Cranmer, E. Gross, O. Vitells, Asymptotic formulae for likelihood-based tests of new physics. *Eur. Phys. J. C* **71**, 1554 (2011). <https://doi.org/10.1140/epjc/s10052-011-1554-0>. arXiv:1007.1727 (Erratum: [10.1140/epjc/s10052-013-2501-z](https://doi.org/10.1140/epjc/s10052-013-2501-z))

CMS Collaboration**Yerevan Physics Institute, Yerevan, Armenia**

A. M. Sirunyan, A. Tumasyan

Institut für Hochenergiephysik, Wien, AustriaW. Adam, F. Ambrogio, E. Asilar, T. Bergauer, J. Brandstetter, M. Dragicevic, J. Erö, A. Escalante Del Valle, M. Flechl, R. Frühwirth¹, V. M. Ghete, J. Hrubec, M. Jeitler¹, N. Krammer, I. Krätschmer, D. Liko, T. Madlener, I. Mikulec, N. Rad, H. Rohringer, J. Schieck¹, R. Schöfbeck, M. Spanring, D. Spitzbart, A. Taurok, W. Waltenberger, J. Wittmann, C.-E. Wulz¹, M. Zarucki**Institute for Nuclear Problems, Minsk, Belarus**

V. Chekhovsky, V. Mossolov, J. Suarez Gonzalez

Universiteit Antwerpen, Antwerpen, Belgium

E. A. De Wolf, D. Di Croce, X. Janssen, J. Lauwers, M. Pieters, H. Van Haevermaet, P. Van Mechelen, N. Van Remortel

Vrije Universiteit Brussel, Brussel, Belgium

S. Abu Zeid, F. Blekman, J. D'Hondt, J. De Clercq, K. Deroover, G. Flouris, D. Lontkovskyi, S. Lowette, I. Marchesini, S. Moortgat, L. Moreels, Q. Python, K. Skovpen, S. Tavernier, W. Van Doninck, P. Van Mulders, I. Van Parijs

Université Libre de Bruxelles, Bruxelles, Belgium

D. Beghin, B. Bilin, H. Brun, B. Clerboux, G. De Lentdecker, H. Delannoy, B. Dorney, G. Fasanella, L. Favart, R. Goldouzian, A. Grebenyuk, A. K. Kalsi, T. Lenzi, J. Luetic, N. Postiau, E. Starling, L. Thomas, C. Vander Velde, P. Vanlaer, D. Vannerom, Q. Wang

Ghent University, Ghent, BelgiumT. Cornelis, D. Dobur, A. Fagot, M. Gul, I. Khvastunov², D. Poyraz, C. Roskas, D. Trocino, M. Tytgat, W. Verbeke, B. Vermassen, M. Vit, N. Zaganidis**Université Catholique de Louvain, Louvain-la-Neuve, Belgium**

H. Bakhshiansohi, O. Bondu, S. Brochet, G. Bruno, C. Caputo, P. David, C. Delaere, M. Delcourt, A. Giammanco, G. Krintiras, V. Lemaître, A. Magitteri, K. Piotrkowski, A. Saggio, M. Vidal Marono, S. Wertz, J. Zobec

Centro Brasileiro de Pesquisas Físicas, Rio de Janeiro, Brazil

F. L. Alves, G. A. Alves, M. Correa Martins Junior, G. Correia Silva, C. Hensel, A. Moraes, M. E. Pol, P. Rebello Teles

Universidade do Estado do Rio de Janeiro, Rio de Janeiro, BrazilE. Belchior Batista Das Chagas, W. Carvalho, J. Chinellato³, E. Coelho, E. M. Da Costa, G. G. Da Silveira⁴, D. De Jesus Damiao, C. De Oliveira Martins, S. Fonseca De Souza, H. Malbouisson, D. Matos Figueiredo, M. Melo De Almeida, C. Mora Herrera, L. Mundim, H. Nogima, W. L. Prado Da Silva, L. J. Sanchez Rosas, A. Santoro, A. Sznajder, M. Thiel, E. J. Tonelli Manganote³, F. Torres Da Silva De Araujo, A. Vilela Pereira**Universidade Estadual Paulista^a, Universidade Federal do ABC^b, São Paulo, Brazil**S. Ahuja^a, C. A. Bernardes^a, L. Calligaris^a, T. R. Fernandez Perez Tomei^a, E. M. Gregores^b, P. G. Mercadante^b, S. F. Novaes^a, Sandra S. Padula^a**Institute for Nuclear Research and Nuclear Energy, Bulgarian Academy of Sciences, Sofia, Bulgaria**

A. Aleksandrov, R. Hadjiiska, P. Iaydjiev, A. Marinov, M. Misheva, M. Rodozov, M. Shopova, G. Sultanov

University of Sofia, Sofia, Bulgaria

A. Dimitrov, L. Litov, B. Pavlov, P. Petkov

Beihang University, Beijing, ChinaW. Fang⁵, X. Gao⁵, L. Yuan**Institute of High Energy Physics, Beijing, China**M. Ahmad, J. G. Bian, G. M. Chen, H. S. Chen, M. Chen, Y. Chen, C. H. Jiang, D. Leggat, H. Liao, Z. Liu, F. Romeo, S. M. Shaheen⁶, A. Spiezia, J. Tao, Z. Wang, E. Yazgan, H. Zhang, S. Zhang⁶, J. Zhao

State Key Laboratory of Nuclear Physics and Technology, Peking University, Beijing, China

Y. Ban, G. Chen, A. Levin, J. Li, L. Li, Q. Li, Y. Mao, S. J. Qian, D. Wang

Tsinghua University, Beijing, China

Y. Wang

Universidad de Los Andes, Bogota, Colombia

C. Avila, A. Cabrera, C. A. Carrillo Montoya, L. F. Chaparro Sierra, C. Florez, C. F. González Hernández, M. A. Segura Delgado

University of Split, Faculty of Electrical Engineering, Mechanical Engineering and Naval Architecture, Split, Croatia

B. Courbon, N. Godinovic, D. Lelas, I. Puljak, T. Sculac

University of Split, Faculty of Science, Split, Croatia

Z. Antunovic, M. Kovac

Institute Rudjer Boskovic, Zagreb, CroatiaV. Brigljevic, D. Ferencek, K. Kadija, B. Mesic, A. Starodumov⁷, T. Susa**University of Cyprus, Nicosia, Cyprus**

M. W. Ather, A. Attikis, A. Ioannou, M. Kolosova, G. Mavromanolakis, J. Mousa, C. Nicolaou, F. Ptochos, P. A. Razis, H. Rykaczewski

Charles University, Prague, Czech RepublicM. Finger⁸, M. Finger Jr.⁸**Escuela Politecnica Nacional, Quito, Ecuador**

E. Ayala

Universidad San Francisco de Quito, Quito, Ecuador

E. Carrera Jarrin

Academy of Scientific Research and Technology of the Arab Republic of Egypt, Egyptian Network of High Energy Physics, Cairo, EgyptH. Abdalla⁹, A. A. Abdelalim^{10,11}, A. Mohamed¹¹**National Institute of Chemical Physics and Biophysics, Tallinn, Estonia**

S. Bhowmik, A. Carvalho Antunes De Oliveira, R. K. Dewanjee, K. Ehataht, M. Kadastik, M. Raidal, C. Veelken

Department of Physics, University of Helsinki, Helsinki, Finland

P. Eerola, H. Kirschenmann, J. Pekkanen, M. Voutilainen

Helsinki Institute of Physics, Helsinki, Finland

J. Havukainen, J. K. Heikkilä, T. Järvinen, V. Karimäki, R. Kinnunen, T. Lampén, K. Lassila-Perini, S. Laurila, S. Lehti, T. Lindén, P. Luukka, T. Mäenpää, H. Siikonen, E. Tuominen, J. Tuominiemi

Lappeenranta University of Technology, Lappeenranta, Finland

T. Tuuva

IRFU, CEA, Université Paris-Saclay, Gif-sur-Yvette, France

M. Besancon, F. Couderc, M. Dejardin, D. Denegri, J. L. Faure, F. Ferri, S. Ganjour, A. Givernaud, P. Gras, G. Hamel de Monchenault, P. Jarry, C. Leloup, E. Locci, J. Malcles, G. Negro, J. Rander, A. Rosowsky, M. Ö. Sahin, M. Titov

Laboratoire Leprince-Ringuet, Ecole polytechnique, CNRS/IN2P3, Université Paris-Saclay, Palaiseau, FranceA. Abdulsalam¹², C. Amendola, I. Antropov, F. Beaudette, P. Busson, C. Charlot, R. Granier de Cassagnac, I. Kucher, A. Lobanov, J. Martin Blanco, C. Martin Perez, M. Nguyen, C. Ochando, G. Ortona, P. Paganini, P. Pigard, J. Rembser, R. Salerno, J. B. Sauvan, Y. Sirois, A. G. Stahl Leitner, A. Zabi, A. Zghiche

Université de Strasbourg, CNRS, IPHC UMR 7178, Strasbourg, France

J.-L. Agram¹³, J. Andrea, D. Bloch, J.-M. Brom, E. C. Chabert, V. Cherepanov, C. Collard, E. Conte¹³, J.-C. Fontaine¹³, D. Gelé, U. Goerlach, M. Jansová, A.-C. Le Bihan, N. Tonon, P. Van Hove

Centre de Calcul de l'Institut National de Physique Nucleaire et de Physique des Particules, CNRS/IN2P3, Villeurbanne, France

S. Gadrat

Université de Lyon, Université Claude Bernard Lyon 1, CNRS-IN2P3, Institut de Physique Nucléaire de Lyon, Villeurbanne, France

S. Beauceron, C. Bernet, G. Boudoul, N. Chanon, R. Chierici, D. Contardo, P. Depasse, H. El Mamouni, J. Fay, L. Finco, S. Gascon, M. Gouzevitch, G. Grenier, B. Ille, F. Lagarde, I. B. Laktineh, H. Lattaud, M. Lethuillier, L. Mirabito, S. Perries, A. Popov¹⁴, V. Sordini, G. Touquet, M. Vander Donckt, S. Viret

Georgian Technical University, Tbilisi, Georgia

T. Toriashvili¹⁵

Tbilisi State University, Tbilisi, Georgia

Z. Tsamalaidze⁸

RWTH Aachen University, I. Physikalisches Institut, Aachen, Germany

C. Autermann, L. Feld, M. K. Kiesel, K. Klein, M. Lipinski, M. Preuten, M. P. Rauch, C. Schomakers, J. Schulz, M. Teroerde, B. Wittmer

RWTH Aachen University, III. Physikalisches Institut A, Aachen, Germany

A. Albert, D. Duchardt, M. Erdmann, S. Erdweg, T. Esch, R. Fischer, S. Ghosh, A. Güth, T. Hebbeker, C. Heidemann, K. Hoepfner, H. Keller, L. Mastrolorenzo, M. Merschmeyer, A. Meyer, P. Millet, S. Mukherjee, T. Pook, M. Radziej, H. Reithler, M. Rieger, A. Schmidt, D. Teyssier, S. Thüer

RWTH Aachen University, III. Physikalisches Institut B, Aachen, Germany

G. Flügge, O. Hlushchenko, T. Kress, T. Müller, A. Nehr Korn, A. Nowack, C. Pistone, O. Pooth, D. Roy, H. Sert, A. Stahl¹⁶

Deutsches Elektronen-Synchrotron, Hamburg, Germany

M. Aldaya Martin, T. Arndt, C. Asawatangtrakuldee, I. Babounikau, K. Beernaert, O. Behnke, U. Behrens, A. Bermúdez Martínez, D. Bertsche, A. A. Bin Anuar, K. Borras¹⁷, V. Botta, A. Campbell, P. Connor, C. Contreras-Campana, V. Danilov, A. De Wit, M. M. Defranchis, C. Diez Pardos, D. Domínguez Damiani, G. Eckerlin, T. Eichhorn, A. Elwood, E. Eren, E. Gallo¹⁸, A. Geiser, J. M. Grados Luyando, A. Grohsjean, M. Guthoff, M. Haranko, A. Harb, J. Hauk, H. Jung, M. Kasemann, J. Keaveney, C. Kleinwort, J. Knolle, D. Krücker, W. Lange, A. Lelek, T. Lenz, J. Leonard, K. Lipka, W. Lohmann¹⁹, R. Mankel, I.-A. Melzer-Pellmann, A. B. Meyer, M. Meyer, M. Missiroli, G. Mittag, J. Mnich, V. Myronenko, S. K. Pflitsch, D. Pitzl, A. Raspereza, M. Savitskyi, P. Saxena, P. Schütze, C. Schwanenberger, R. Shevchenko, A. Singh, H. Tholen, O. Turkot, A. Vagnerini, G. P. Van Onsem, R. Walsh, Y. Wen, K. Wichmann, C. Wissing, O. Zenaiev

University of Hamburg, Hamburg, Germany

R. Aggleton, S. Bein, L. Benato, A. Benecke, V. Blobel, T. Dreyer, A. Ebrahimi, E. Garutti, D. Gonzalez, P. Gunnellini, J. Haller, A. Hinzmann, A. Karavdina, G. Kasieczka, R. Klanner, R. Kogler, N. Kovalchuk, S. Kurz, V. Kutzner, J. Lange, D. Marconi, J. Multhaupt, M. Niedziela, C. E. N. Niemeyer, D. Nowatschin, A. Perieanu, A. Reimers, O. Rieger, C. Scharf, P. Schleper, S. Schumann, J. Schwandt, J. Sonneveld, H. Stadie, G. Steinbrück, F. M. Stober, M. Stöver, A. Vanhoefer, B. Vormwald, I. Zoi

Karlsruher Institut fuer Technologie, Karlsruhe, Germany

M. Akbiyik, C. Barth, M. Baselga, S. Baur, E. Butz, R. Caspart, T. Chwalek, F. Colombo, W. De Boer, A. Dierlamm, K. El Morabit, N. Faltermann, B. Freund, M. Giffels, M. A. Harrendorf, F. Hartmann¹⁶, S. M. Heindl, U. Husemann, I. Katkov¹⁴, S. Kudella, S. Mitra, M. U. Mozer, Th. Müller, M. Musich, M. Plagge, G. Quast, K. Rabbertz, M. Schröder, I. Shvetsov, H. J. Simonis, R. Ulrich, S. Wayand, M. Weber, T. Weiler, C. Wöhrmann, R. Wolf

Institute of Nuclear and Particle Physics (INPP), NCSR Demokritos, Aghia Paraskevi, Greece

G. Anagnostou, G. Daskalakis, T. Geralis, A. Kyriakis, D. Loukas, G. Paspalaki

National and Kapodistrian University of Athens, Athens, Greece

A. Agapitos, G. Karathanasis, P. Kontaxakis, A. Panagiotou, I. Papavergou, N. Saoulidou, E. Tziaferi, K. Vellidis

National Technical University of Athens, Athens, Greece

K. Kousouris, I. Papakrivopoulos, G. Tsipolitis

University of Ioánnina, Ioánnina, Greece

I. Evangelou, C. Foudas, P. Giannios, P. Katsoulis, P. Kokkas, S. Mallios, N. Manthos, I. Papadopoulos, E. Paradas, J. Strologas, F. A. Triantis, D. Tsitsonis

MTA-ELTE Lendület CMS Particle and Nuclear Physics Group, Eötvös Loránd University, Budapest, Hungary

M. Bartók²⁰, M. Csanad, N. Filipovic, P. Major, M. I. Nagy, G. Pasztor, O. Surányi, G. I. Veres

Wigner Research Centre for Physics, Budapest, Hungary

G. Bencze, C. Hajdu, D. Horvath²¹, Á. Hunyadi, F. Sikler, T. Á. Vámi, V. Veszpremi, G. Vesztergombi[†]

Institute of Nuclear Research ATOMKI, Debrecen, Hungary

N. Beni, S. Czellar, J. Karancsi²⁰, A. Makovec, J. Molnar, Z. Szillasi

Institute of Physics, University of Debrecen, Debrecen, Hungary

P. Raics, Z. L. Trocsanyi, B. Ujvari

Indian Institute of Science (IISc), Bangalore, India

S. Choudhury, J. R. Komaragiri, P. C. Tiwari

National Institute of Science Education and Research, HBNI, Bhubaneswar, India

S. Bahinipati²³, C. Kar, P. Mal, K. Mandal, A. Nayak²⁴, D. K. Sahoo²³, S. K. Swain

Panjab University, Chandigarh, India

S. Bansal, S. B. Beri, V. Bhatnagar, S. Chauhan, R. Chawla, N. Dhingra, R. Gupta, A. Kaur, M. Kaur, S. Kaur, P. Kumari, M. Lohan, A. Mehta, K. Sandeep, S. Sharma, J. B. Singh, A. K. Viridi, G. Walia

University of Delhi, Delhi, India

A. Bhardwaj, B. C. Choudhary, R. B. Garg, M. Gola, S. Keshri, Ashok Kumar, S. Malhotra, M. Naimuddin, P. Priyanka, K. Ranjan, Aashaq Shah, R. Sharma

Saha Institute of Nuclear Physics, HBNI, Kolkata, India

R. Bhardwaj²⁵, M. Bharti²⁵, R. Bhattacharya, S. Bhattacharya, U. Bhawandeep²⁵, D. Bhowmik, S. Dey, S. Dutt²⁵, S. Dutta, S. Ghosh, K. Mondal, S. Nandan, A. Purohit, P. K. Rout, A. Roy, S. Roy Chowdhury, G. Saha, S. Sarkar, M. Sharan, B. Singh²⁵, S. Thakur²⁵

Indian Institute of Technology Madras, Chennai, India

P. K. Behera

Bhabha Atomic Research Centre, Mumbai, India

R. Chudasama, D. Dutta, V. Jha, V. Kumar, P. K. Netrakanti, L. M. Pant, P. Shukla

Tata Institute of Fundamental Research-A, Mumbai, India

T. Aziz, M. A. Bhat, S. Dugad, G. B. Mohanty, N. Sur, B. Sutar, RavindraKumar Verma

Tata Institute of Fundamental Research-B, Mumbai, India

S. Banerjee, S. Bhattacharya, S. Chatterjee, P. Das, M. Guchait, Sa. Jain, S. Karmakar, S. Kumar, M. Maity²⁶, G. Majumder, K. Mazumdar, N. Sahoo, T. Sarkar²⁶

Indian Institute of Science Education and Research (IISER), Pune, India

S. Chauhan, S. Dube, V. Hegde, A. Kapoor, K. Kotheekar, S. Pandey, A. Rane, A. Rastogi, S. Sharma

Institute for Research in Fundamental Sciences (IPM), Tehran, Iran

S. Chenarani²⁷, E. Eskandari Tadavani, S. M. Etesami²⁷, M. Khakzad, M. Mohammadi Najafabadi, M. Naseri, F. Rezaei Hosseinabadi, B. Safarzadeh²⁸, M. Zeinali

University College Dublin, Dublin, Ireland

M. Felcini, M. Grunewald

INFN Sezione di Bari^a, Università di Bari^b, Politecnico di Bari^c, Bari, Italy

M. Abbrescia^{a,b}, C. Calabria^{a,b}, A. Colaleo^a, D. Creanza^{a,c}, L. Cristella^{a,b}, N. De Filippis^{a,c}, M. De Palma^{a,b},
 A. Di Florio^{a,b}, F. Errico^{a,b}, L. Fiore^a, A. Gelmi^{a,b}, G. Iaselli^{a,c}, M. Ince^{a,b}, S. Lezki^{a,b}, G. Maggi^{a,c}, M. Maggi^a,
 G. Miniello^{a,b}, S. My^{a,b}, S. Nuzzo^{a,b}, A. Pompili^{a,b}, G. Pugliese^{a,c}, R. Radogna^a, A. Ranieri^a, G. Selvaggi^{a,b},
 A. Sharma^a, L. Silvestris^a, R. Venditti^a, P. Verwilligen^a, G. Zito^a

INFN Sezione di Bologna^a, Università di Bologna^b, Bologna, Italy

G. Abbiendi^a, C. Battilana^{a,b}, D. Bonacorsi^{a,b}, L. Borgonovi^{a,b}, S. Braibant-Giacomelli^{a,b}, R. Campanini^{a,b},
 P. Capiluppi^{a,b}, A. Castro^{a,b}, F. R. Cavallo^a, S. S. Chhibra^{a,b}, C. Ciocca^a, G. Codispoti^{a,b}, M. Cuffiani^{a,b},
 G. M. Dallavalle^a, F. Fabbri^a, A. Fanfani^{a,b}, E. Fontanesi, P. Giacomelli^a, C. Grandi^a, L. Guiducci^{a,b}, F. Iemmi^{a,b},
 S. Lo Meo^a, S. Marcellini^a, G. Masetti^a, A. Montanari^a, F. L. Navarria^{a,b}, A. Perrotta^a, F. Primavera^{a,b,16}, T. Rovelli^{a,b},
 G. P. Siroli^{a,b}, N. Tosi^a

INFN Sezione di Catania^a, Università di Catania^b, Catania, ItalyS. Albergo^{a,b}, A. Di Mattia^a, R. Potenza^{a,b}, A. Tricomi^{a,b}, C. Tuve^{a,b}**INFN Sezione di Firenze^a, Università di Firenze^b, Firenze, Italy**

G. Barbagli^a, K. Chatterjee^{a,b}, V. Ciulli^{a,b}, C. Civinini^a, R. D'Alessandro^{a,b}, E. Focardi^{a,b}, G. Latino, P. Lenzi^{a,b},
 M. Meschini^a, S. Paoletti^a, L. Russo^{a,29}, G. Sguazzoni^a, D. Strom^a, L. Viliani^a

INFN Laboratori Nazionali di Frascati, Frascati, Italy

L. Benussi, S. Bianco, F. Fabbri, D. Piccolo

INFN Sezione di Genova^a, Università di Genova^b, Genova, ItalyF. Ferro^a, R. Mulargia^{a,b}, F. Ravera^{a,b}, E. Robutti^a, S. Tosi^{a,b}**INFN Sezione di Milano-Bicocca^a, Università di Milano-Bicocca^b, Milan, Italy**

A. Benaglia^a, A. Beschi^b, F. Brivio^{a,b}, V. Ciriolo^{a,b,16}, S. Di Guida^{a,d,16}, M. E. Dinardo^{a,b}, S. Fiorendi^{a,b}, S. Gennai^a,
 A. Ghezzi^{a,b}, P. Govoni^{a,b}, M. Malberti^{a,b}, S. Malvezzi^a, D. Menasce^a, F. Monti^a, L. Moroni^a, M. Paganoni^{a,b},
 D. Pedrini^a, S. Ragazzi^{a,b}, T. Tabarelli de Fatis^{a,b}, D. Zuolo^{a,b}

INFN Sezione di Napoli^a, Università di Napoli 'Federico II'^b, Napoli, Italy, Università della Basilicata^c, Potenza, Italy, Università G. Marconi^d, Rome, Italy

S. Buontempo^a, N. Cavallo^{a,c}, A. De Iorio^{a,b}, A. Di Crescenzo^{a,b}, F. Fabozzi^{a,c}, F. Fienga^a, G. Galati^a, A. O. M. Iorio^{a,b},
 W. A. Khan^a, L. Lista^a, S. Meola^{a,d,16}, P. Paolucci^{a,16}, C. Sciacca^{a,b}, E. Voevodina^{a,b}

INFN Sezione di Padova^a, Università di Padova^b, Padova, Italy, Università di Trento^c, Trento, Italy

P. Azzi^a, N. Bacchetta^a, D. Bisello^{a,b}, A. Boletti^{a,b}, A. Bragagnolo, R. Carlin^{a,b}, P. Checchia^a, M. Dall'Osso^{a,b},
 P. De Castro Manzano^a, T. Dorigo^a, U. Dosselli^a, F. Gasparini^{a,b}, U. Gasparini^{a,b}, A. Gozzelino^a, S. Y. Hoh,
 S. Lacaprara^a, P. Lujan, M. Margoni^{a,b}, A. T. Meneguzzo^{a,b}, J. Pazzini^{a,b}, N. Pozzobon^{a,b}, P. Ronchese^{a,b}, R. Rossin^{a,b},
 F. Simonetto^{a,b}, A. Tiko, E. Torassa^a, M. Tosi^{a,b}, S. Ventura^a, M. Zanetti^{a,b}

INFN Sezione di Pavia^a, Università di Pavia^b, Pavia, Italy

A. Braghieri^a, A. Magnani^a, P. Montagna^{a,b}, S. P. Ratti^{a,b}, V. Re^a, M. Ressegotti^{a,b}, C. Riccardi^{a,b}, P. Salvini^a, I. Vai^{a,b},
 P. Vitulo^{a,b}

INFN Sezione di Perugia^a, Università di Perugia^b, Perugia, Italy

M. Biasini^{a,b}, G. M. Bilei^a, C. Cecchi^{a,b}, D. Ciangottini^{a,b}, L. Fanò^{a,b}, P. Lariccia^{a,b}, R. Leonardi^{a,b}, E. Manoni^a,
 G. Mantovani^{a,b}, V. Mariani^{a,b}, M. Menichelli^a, A. Rossi^{a,b}, A. Santocchia^{a,b}, D. Spiga^a

INFN Sezione di Pisa^a, Università di Pisa^b, Scuola Normale Superiore di Pisa^c, Pisa, Italy

K. Androsov^a, P. Azzurri^a, G. Bagliesi^a, L. Bianchini^a, T. Boccali^a, L. Borrello, R. Castaldi^a, M. A. Ciocci^{a,b},
 R. Dell'Orso^a, G. Fedi^a, F. Fiori^{a,c}, L. Giannini^{a,c}, A. Giassi^a, M. T. Grippo^a, F. Ligabue^{a,c}, E. Manca^{a,c}, G. Mandorli^{a,c},
 A. Messineo^{a,b}, F. Palla^a, A. Rizzi^{a,b}, G. Rolandi³⁰, P. Spagnolo^a, R. Tenchini^a, G. Tonelli^{a,b}, A. Venturi^a, P. G. Verdini^a

INFN Sezione di Roma^a, Sapienza Università di Roma^b, Rome, Italy

L. Barone^{a,b}, F. Cavallari^a, M. Cipriani^{a,b}, D. Del Re^{a,b}, E. Di Marco^{a,b}, M. Diemoz^a, S. Gelli^{a,b}, E. Longo^{a,b}, B. Marzocchi^{a,b}, P. Meridiani^a, G. Organtini^{a,b}, F. Pandolfi^a, R. Paramatti^{a,b}, F. Preiato^{a,b}, S. Rahatlou^{a,b}, C. Rovelli^a, F. Santanastasio^{a,b}

INFN Sezione di Torino^a, Università di Torino^b, Torino, Italy, Università del Piemonte Orientale^c, Novara, Italy

N. Amapane^{a,b}, R. Arcidiacono^{a,c}, S. Argiro^{a,b}, M. Arneodo^{a,c}, N. Bartosik^a, R. Bellan^{a,b}, C. Biino^a, A. Cappati^{a,b}, N. Cartiglia^a, F. Cenna^{a,b}, S. Cometti^a, M. Costa^{a,b}, R. Covarelli^{a,b}, N. Demaria^a, B. Kiani^{a,b}, C. Mariotti^a, S. Maselli^a, E. Migliore^{a,b}, V. Monaco^{a,b}, E. Monteil^{a,b}, M. Monteno^a, M. M. Obertino^{a,b}, L. Pacher^{a,b}, N. Pastrone^a, M. Pelliccioni^a, G. L. Pinna Angioni^{a,b}, A. Romero^{a,b}, M. Ruspai^{a,c}, R. Sacchi^{a,b}, R. Salvatico^{a,b}, K. Shchelina^{a,b}, V. Sola^a, A. Solano^{a,b}, D. Soldi^{a,b}, A. Staiano^a

INFN Sezione di Trieste^a, Università di Trieste^b, Trieste, Italy

S. Belforte^a, V. Candelise^{a,b}, M. Casarsa^a, F. Cossutti^a, A. Da Rold^{a,b}, G. Della Ricca^{a,b}, F. Vazzoler^{a,b}, A. Zanetti^a

Kyungpook National University, Daegu, Korea

D. H. Kim, G. N. Kim, M. S. Kim, J. Lee, S. Lee, S. W. Lee, C. S. Moon, Y. D. Oh, S. I. Pak, S. Sekmen, D. C. Son, Y. C. Yang

Chonnam National University, Institute for Universe and Elementary Particles, Kwangju, Korea

H. Kim, D. H. Moon, G. Oh

Hanyang University, Seoul, Korea

B. Francois, J. Goh³¹, T. J. Kim

Korea University, Seoul, Korea

S. Cho, S. Choi, Y. Go, D. Gyun, S. Ha, B. Hong, Y. Jo, K. Lee, K. S. Lee, S. Lee, J. Lim, S. K. Park, Y. Roh

Sejong University, Seoul, Korea

H. S. Kim

Seoul National University, Seoul, Korea

J. Almond, J. Kim, J. S. Kim, H. Lee, K. Lee, K. Nam, S. B. Oh, B. C. Radburn-Smith, S. h. Seo, U. K. Yang, H. D. Yoo, G. B. Yu

University of Seoul, Seoul, Korea

D. Jeon, H. Kim, J. H. Kim, J. S. H. Lee, I. C. Park

Sungkyunkwan University, Suwon, Korea

Y. Choi, C. Hwang, J. Lee, I. Yu

Vilnius University, Vilnius, Lithuania

V. Dudenas, A. Juodagalvis, J. Vaitkus

National Centre for Particle Physics, Universiti Malaya, Kuala Lumpur, Malaysia

I. Ahmed, Z. A. Ibrahim, M. A. B. Md Ali³², F. Mohamad Idris³³, W. A. T. Wan Abdullah, M. N. Yusli, Z. Zolkapli

Universidad de Sonora (UNISON), Hermosillo, Mexico

J. F. Benitez, A. Castaneda Hernandez, J. A. Murillo Quijada

Centro de Investigacion y de Estudios Avanzados del IPN, Mexico City, Mexico

H. Castilla-Valdez, E. De La Cruz-Burelo, M. C. Duran-Osuna, I. Heredia-De La Cruz³⁴, R. Lopez-Fernandez, J. Mejia Guisao, R. I. Rabadan-Trejo, M. Ramirez-Garcia, G. Ramirez-Sanchez, R. Reyes-Almanza, A. Sanchez-Hernandez

Universidad Iberoamericana, Mexico City, Mexico

S. Carrillo Moreno, C. Oropeza Barrera, F. Vazquez Valencia

Benemerita Universidad Autonoma de Puebla, Puebla, Mexico

J. Eysermans, I. Pedraza, H. A. Salazar Ibarguen, C. Uribe Estrada

Universidad Autónoma de San Luis Potosí, San Luis Potosí, Mexico

A. Morelos Pineda

University of Auckland, Auckland, New Zealand

D. Krofcheck

University of Canterbury, Christchurch, New Zealand

S. Bheesette, P. H. Butler

National Centre for Physics, Quaid-I-Azam University, Islamabad, Pakistan

A. Ahmad, M. Ahmad, M. I. Asghar, Q. Hassan, H. R. Hoorani, A. Saddique, M. A. Shah, M. Shoaib, M. Waqas

National Centre for Nuclear Research, Swierk, Poland

H. Bialkowska, M. Bluj, B. Boimska, T. Frueboes, M. Górski, M. Kazana, M. Szeleper, P. Traczyk, P. Zalewski

Institute of Experimental Physics, Faculty of Physics, University of Warsaw, Warsaw, PolandK. Bunkowski, A. Byszuk³⁵, K. Doroba, A. Kalinowski, M. Konecki, J. Krolikowski, M. Misiura, M. Olszewski, A. Pyskir, M. Walczak**Laboratório de Instrumentação e Física Experimental de Partículas, Lisboa, Portugal**

M. Araujo, P. Bargassa, C. Beirão Da Cruz E Silva, A. Di Francesco, P. Faccioli, B. Galinhas, M. Gallinaro, J. Hollar, N. Leonardo, J. Seixas, G. Strong, O. Toldaiev, J. Varela

Joint Institute for Nuclear Research, Dubna, RussiaS. Afanasiev, P. Bunin, M. Gavrilenko, I. Golutvin, I. Gorbunov, A. Kamenev, V. Karjavine, A. Lanev, A. Malakhov, V. Matveev^{36,37}, V. V. Mitsyn, P. Moisezenz, V. Palichik, V. Pereygin, S. Shmatov, S. Shulha, N. Skatchkov, V. Smirnov, N. Voytishin, A. Zarubin**Petersburg Nuclear Physics Institute, Gatchina (St. Petersburg), Russia**V. Golovtsov, Y. Ivanov, V. Kim³⁸, E. Kuznetsova³⁹, P. Levchenko, V. Murzin, V. Oreshkin, I. Smirnov, D. Sosnov, V. Sulimov, L. Uvarov, S. Vavilov, A. Vorobyev**Institute for Nuclear Research, Moscow, Russia**

Yu. Andreev, A. Dermenev, S. Gninenko, N. Golubev, A. Karneyeu, M. Kirsanov, N. Krasnikov, A. Pashenkov, D. Tlisov, A. Toropin

Institute for Theoretical and Experimental Physics, Moscow, Russia

V. Epshteyn, V. Gavrilov, N. Lychkovskaya, V. Popov, I. Pozdnyakov, G. Safronov, A. Spiridonov, A. Stepenov, V. Stolin, M. Toms, E. Vlasov, A. Zhokin

Moscow Institute of Physics and Technology, Moscow, Russia

T. Aushev

National Research Nuclear University 'Moscow Engineering Physics Institute' (MEPhI), Moscow, RussiaR. Chistov⁴⁰, M. Danilov⁴⁰, P. Parygin, D. Philippov, S. Polikarpov⁴⁰, E. Tarkovskii**P.N. Lebedev Physical Institute, Moscow, Russia**V. Andreev, M. Azarkin, I. Dremin³⁷, M. Kirakosyan, A. Terkulov**Skobeltsyn Institute of Nuclear Physics, Lomonosov Moscow State University, Moscow, Russia**A. Baskakov, A. Belyaev, E. Boos, M. Dubinin⁴¹, L. Dudko, A. Ershov, A. Gribushin, V. Klyukhin, O. Kodolova, I. Lokhtin, I. Miagkov, S. Obraztsov, S. Petrushanko, V. Savrin, A. Snigirev**Novosibirsk State University (NSU), Novosibirsk, Russia**A. Barnyakov⁴², V. Blinov⁴², T. Dimova⁴², L. Kardapoltsev⁴², Y. Skovpen⁴²**Institute for High Energy Physics of National Research Centre 'Kurchatov Institute', Protvino, Russia**

I. Azhgirey, I. Bayshev, S. Bitioukov, D. Elumakhov, A. Godizov, V. Kachanov, A. Kalinin, D. Konstantinov, P. Mandrik, V. Petrov, R. Ryutin, S. Slabospitskii, A. Sobol, S. Troshin, N. Tyurin, A. Uzunian, A. Volkov

National Research Tomsk Polytechnic University, Tomsk, Russia

A. Babaev, S. Baidali, V. Okhotnikov

University of Belgrade: Faculty of Physics and VINCA Institute of Nuclear Sciences, Belgrade, SerbiaP. Adzic⁴³, P. Cirkovic, D. Devetak, M. Dordevic, J. Milosevic**Centro de Investigaciones Energéticas Medioambientales y Tecnológicas (CIEMAT), Madrid, Spain**

J. Alcaraz Maestre, A. Álvarez Fernández, I. Bachiller, M. Barrio Luna, J. A. Brochero Cifuentes, M. Cerrada, N. Colino, B. De La Cruz, A. Delgado Peris, C. Fernandez Bedoya, J. P. Fernández Ramos, J. Flix, M. C. Fouz, O. Gonzalez Lopez, S. Goy Lopez, J. M. Hernandez, M. I. Josa, D. Moran, A. Pérez-Calero Yzquierdo, J. Puerta Pelayo, I. Redondo, L. Romero, M. S. Soares, A. Triossi

Universidad Autónoma de Madrid, Madrid, Spain

C. Albajar, J. F. de Trocóniz

Universidad de Oviedo, Oviedo, Spain

J. Cuevas, C. Erice, J. Fernandez Menendez, S. Folgueras, I. Gonzalez Caballero, J. R. González Fernández, E. Palencia Cortezon, V. Rodríguez Bouza, S. Sanchez Cruz, P. Vischia, J. M. Vizán García

Instituto de Física de Cantabria (IFCA), CSIC-Universidad de Cantabria, Santander, Spain

I. J. Cabrillo, A. Calderon, B. Chazin Quero, J. Duarte Campderros, M. Fernandez, P. J. Fernández Manteca, A. García Alonso, J. Garcia-Ferrero, G. Gomez, A. Lopez Virto, J. Marco, C. Martinez Rivero, P. Martinez Ruiz del Arbol, F. Matorras, J. Piedra Gomez, C. Prieels, T. Rodrigo, A. Ruiz-Jimeno, L. Scodellaro, N. Trevisani, I. Vila, R. Vilar Cortabitarte

University of Ruhuna, Department of Physics, Matara, Sri Lanka

N. Wickramage

CERN, European Organization for Nuclear Research, Geneva, SwitzerlandD. Abbaneo, B. Akgun, E. Auffray, G. Auzinger, P. Baillon, A. H. Ball, D. Barney, J. Bendavid, M. Bianco, A. Bocci, C. Botta, E. Brondolin, T. Camporesi, M. Cepeda, G. Cerminara, E. Chapon, Y. Chen, G. Cucciati, D. d'Enterria, A. Dabrowski, N. Daci, V. Daponte, A. David, A. De Roeck, N. Deelen, M. Dobson, M. Dünser, N. Dupont, A. Elliott-Peisert, P. Everaerts, F. Fallavollita⁴⁴, D. Fasanella, G. Franzoni, J. Fulcher, W. Funk, D. Gigi, A. Gilbert, K. Gill, F. Glege, M. Gruchala, M. Guilbaud, D. Gulhan, J. Hegeman, C. Heidegger, V. Innocente, A. Jafari, P. Janot, O. Karacheban¹⁹, J. Kieseler, A. Kornmayer, M. Krammer¹, C. Lange, P. Lecoq, C. Lourenço, L. Malgeri, M. Mannelli, A. Massironi, F. Meijers, J. A. Merlin, S. Mersi, E. Meschi, P. Milenovic⁴⁵, F. Moortgat, M. Mulders, J. Ngadiuba, S. Nourbakhsh, S. Orfanelli, L. Orsini, F. Pantaleo¹⁶, L. Pape, E. Perez, M. Peruzzi, A. Petrilli, G. Petrucciani, A. Pfeiffer, M. Pierini, F. M. Pitters, D. Rabady, A. Racz, T. Reis, M. Rovere, H. Sakulin, C. Schäfer, C. Schwick, M. Selvaggi, A. Sharma, P. Silva, P. Sphicas⁴⁶, A. Stakia, J. Stegmann, D. Treille, A. Tsirou, V. Veckalns⁴⁷, M. Verzetti, W. D. Zeuner**Paul Scherrer Institut, Villigen, Switzerland**L. Caminada⁴⁸, K. Deiters, W. Erdmann, R. Horisberger, Q. Ingram, H. C. Kaestli, D. Kotlinski, U. Langenegger, T. Rohe, S. A. Wiederkehr**ETH Zurich - Institute for Particle Physics and Astrophysics (IPA), Zurich, Switzerland**

M. Backhaus, L. Bäni, P. Berger, N. Chernyavskaya, G. Dissertori, M. Dittmar, M. Donegà, C. Dorfer, T. A. Gómez Espinosa, C. Grab, D. Hits, T. Klijnsma, W. Lustermann, R. A. Manzoni, M. Marionneau, M. T. Meinhard, F. Micheli, P. Musella, F. Nessi-Tedaldi, J. Pata, F. Pauss, G. Perrin, L. Perrozzi, S. Pigazzini, M. Quittnat, C. Reissel, D. Ruini, D. A. Sanz Becerra, M. Schönenberger, L. Shchutska, V. R. Tavolaro, K. Theofilatos, M. L. Vesterbacka Olsson, R. Wallny, D. H. Zhu

Universität Zürich, Zurich, SwitzerlandT. K. Aarrestad, C. Amsler⁴⁹, D. Brzhechko, M. F. Canelli, A. De Cosa, R. Del Burgo, S. Donato, C. Galloni, T. Hreus, B. Kilminster, S. Leontsinis, I. Neutelings, G. Rauco, P. Robmann, D. Salerno, K. Schweiger, C. Seitz, Y. Takahashi, A. Zucchetta**National Central University, Chung-Li, Taiwan**

T. H. Doan, R. Khurana, C. M. Kuo, W. Lin, A. Pozdnyakov, S. S. Yu

National Taiwan University (NTU), Taipei, Taiwan

P. Chang, Y. Chao, K. F. Chen, P. H. Chen, W.-S. Hou, Arun Kumar, Y. F. Liu, R.-S. Lu, E. Paganis, A. Psallidas, A. Steen

Chulalongkorn University, Faculty of Science, Department of Physics, Bangkok, Thailand

B. Asavapibhop, N. Srimanobhas, N. Suwonjandee

Çukurova University, Physics Department, Science and Art Faculty, Adana, Turkey

A. Bat, F. Boran, S. Damarseckin, Z. S. Demiroglu, F. Dolek, C. Dozen, I. Dumanoglu, S. Girgis, G. Gokbulut, Y. Guler, E. Gurpinar, I. Hos⁵⁰, C. Isik, E. E. Kangal⁵¹, O. Kara, A. Kayis Topaksu, U. Kiminsu, M. Oglakci, G. Onengut, K. Ozdemir⁵², S. Ozturk⁵³, D. Sunar Cerci⁵⁴, B. Tali⁵⁴, U. G. Tok, H. Topakli⁵³, S. Turkcapar, I. S. Zorbakir, C. Zorbilmez

Middle East Technical University, Physics Department, Ankara, Turkey

B. Isildak⁵⁵, G. Karapinar⁵⁶, M. Yalvac, M. Zeyrek

Bogazici University, Istanbul, Turkey

I. O. Atakisi, E. Gülmez, M. Kaya⁵⁷, O. Kaya⁵⁸, S. Ozkorucuklu⁵⁹, S. Tekten, E. A. Yetkin⁶⁰

Istanbul Technical University, Istanbul, Turkey

M. N. Agaras, A. Cakir, K. Cankocak, Y. Komurcu, S. Sen⁶¹

Institute for Scintillation Materials of National Academy of Science of Ukraine, Kharkov, Ukraine

B. Grynyov

National Scientific Center, Kharkov Institute of Physics and Technology, Kharkov, Ukraine

L. Levchuk

University of Bristol, Bristol, United Kingdom

F. Ball, J. J. Brooke, D. Burns, E. Clement, D. Cussans, O. Davignon, H. Flacher, J. Goldstein, G. P. Heath, H. F. Heath, L. Kreczko, D. M. Newbold⁶², S. Paramesvaran, B. Penning, T. Sakuma, D. Smith, V. J. Smith, J. Taylor, A. Titterton

Rutherford Appleton Laboratory, Didcot, United Kingdom

K. W. Bell, A. Belyaev⁶³, C. Brew, R. M. Brown, D. Cieri, D. J. A. Cockerill, J. A. Coughlan, K. Harder, S. Harper, J. Linacre, K. Manolopoulos, E. Olaiya, D. Petyt, C. H. Shepherd-Themistocleous, A. Thea, I. R. Tomalin, T. Williams, W. J. Womersley

Imperial College, London, United Kingdom

R. Bainbridge, P. Bloch, J. Borg, S. Breeze, O. Buchmuller, A. Bundock, D. Colling, P. Dauncey, G. Davies, M. Della Negra, R. Di Maria, G. Hall, G. Iles, T. James, M. Komm, C. Laner, L. Lyons, A.-M. Magnan, S. Malik, A. Martelli, J. Nash⁶⁴, A. Nikitenko⁷, V. Palladino, M. Pesaresi, D. M. Raymond, A. Richards, A. Rose, E. Scott, C. Seez, A. Shtipliyski, G. Singh, M. Stoye, T. Strebler, S. Summers, A. Tapper, K. Uchida, T. Virdee¹⁶, N. Wardle, D. Winterbottom, J. Wright, S. C. Zenz

Brunel University, Uxbridge, United Kingdom

J. E. Cole, P. R. Hobson, A. Khan, P. Kyberd, C. K. Mackay, A. Morton, I. D. Reid, L. Teodorescu, S. Zahid

Baylor University, Waco, USA

K. Call, J. Dittmann, K. Hatakeyama, H. Liu, C. Madrid, B. McMaster, N. Pastika, C. Smith

Catholic University of America, Washington DC, USA

R. Bartek, A. Dominguez

The University of Alabama, Tuscaloosa, USA

A. Buccilli, S. I. Cooper, C. Henderson, P. Rumerio, C. West

Boston University, Boston, USA

D. Arcaro, T. Bose, D. Gastler, D. Pinna, D. Rankin, C. Richardson, J. Rohlf, L. Sulak, D. Zou

Brown University, Providence, USA

G. Benelli, X. Coubez, D. Cutts, M. Hadley, J. Hakala, U. Heintz, J. M. Hogan⁶⁵, K. H. M. Kwok, E. Laird, G. Landsberg, J. Lee, Z. Mao, M. Narain, S. Sagir⁶⁶, R. Syarif, E. Usai, D. Yu

University of California, Davis, Davis, USA

R. Band, C. Brainerd, R. Breedon, D. Burns, M. Calderon De La Barca Sanchez, M. Chertok, J. Conway, R. Conway, P. T. Cox, R. Erbacher, C. Flores, G. Funk, W. Ko, O. Kukral, R. Lander, M. Mulhearn, D. Pellett, J. Pilot, S. Shalhout, M. Shi, D. Stolp, D. Taylor, K. Tos, M. Tripathi, Z. Wang, F. Zhang

University of California, Los Angeles, USA

M. Bachtis, C. Bravo, R. Cousins, A. Dasgupta, A. Florent, J. Hauser, M. Ignatenko, N. Mccoll, S. Regnard, D. Saltzberg, C. Schnaible, V. Valuev

University of California, Riverside, Riverside, USA

E. Bouvier, K. Burt, R. Clare, J. W. Gary, S. M. A. Ghiasi Shirazi, G. Hanson, G. Karapostoli, E. Kennedy, F. Lacroix, O. R. Long, M. Olmedo Negrete, M. I. Paneva, W. Si, L. Wang, H. Wei, S. Wimpenny, B. R. Yates

University of California, San Diego, La Jolla, USA

J. G. Branson, P. Chang, S. Cittolin, M. Derdzinski, R. Gerosa, D. Gilbert, B. Hashemi, A. Holzner, D. Klein, G. Kole, V. Krutelyov, J. Letts, M. Masciovecchio, D. Olivito, S. Padhi, M. Pieri, M. Sani, V. Sharma, S. Simon, M. Tadel, A. Vartak, S. Wasserbaech⁶⁷, J. Wood, F. Würthwein, A. Yagil, G. Zevi Della Porta

University of California, Santa Barbara - Department of Physics, Santa Barbara, USA

N. Amin, R. Bhandari, C. Campagnari, M. Citron, V. Dutta, M. Franco Sevilla, L. Gouskos, R. Heller, J. Incandela, A. Ovcharova, H. Qu, J. Richman, D. Stuart, I. Suarez, S. Wang, J. Yoo

California Institute of Technology, Pasadena, USA

D. Anderson, A. Bornheim, J. M. Lawhorn, N. Lu, H. B. Newman, T. Q. Nguyen, M. Spiropulu, J. R. Vlimant, R. Wilkinson, S. Xie, Z. Zhang, R. Y. Zhu

Carnegie Mellon University, Pittsburgh, USA

M. B. Andrews, T. Ferguson, T. Mudholkar, M. Paulini, M. Sun, I. Vorobiev, M. Weinberg

University of Colorado Boulder, Boulder, USA

J. P. Cumalat, W. T. Ford, F. Jensen, A. Johnson, E. MacDonald, T. Mulholland, R. Patel, A. Perloff, K. Stenson, K. A. Ulmer, S. R. Wagner

Cornell University, Ithaca, USA

J. Alexander, J. Chaves, Y. Cheng, J. Chu, A. Datta, K. Mcdermott, N. Mirman, J. R. Patterson, D. Quach, A. Rinkevicius, A. Ryd, L. Skinnari, L. Soffi, S. M. Tan, Z. Tao, J. Thom, J. Tucker, P. Wittich, M. Zientek

Fermi National Accelerator Laboratory, Batavia, USA

S. Abdullin, M. Albrow, M. Alyari, G. Apollinari, A. Apresyan, A. Apyan, S. Banerjee, L. A. T. Bauerdick, A. Beretvas, J. Berryhill, P. C. Bhat, K. Burkett, J. N. Butler, A. Canepa, G. B. Cerati, H. W. K. Cheung, F. Chlebana, M. Cremonesi, J. Duarte, V. D. Elvira, J. Freeman, Z. Gecse, E. Gottschalk, L. Gray, D. Green, S. Grünendahl, O. Gutsche, J. Hanlon, R. M. Harris, S. Hasegawa, J. Hirschauer, Z. Hu, B. Jayatilaka, S. Jindariani, M. Johnson, U. Joshi, B. Klima, M. J. Kortelainen, B. Kreis, S. Lammel, D. Lincoln, R. Lipton, M. Liu, T. Liu, J. Lykken, K. Maeshima, J. M. Marraffino, D. Mason, P. McBride, P. Merkel, S. Mrenna, S. Nahn, V. O'Dell, K. Pedro, C. Pena, O. Prokofyev, G. Rakness, L. Ristori, A. Savoy-Navarro⁶⁸, B. Schneider, E. Sexton-Kennedy, A. Soha, W. J. Spalding, L. Spiegel, S. Stoynev, J. Strait, N. Strobbe, L. Taylor, S. Tkaczyk, N. V. Tran, L. Uplegger, E. W. Vaandering, C. Vernieri, M. Verzocchi, R. Vidal, M. Wang, H. A. Weber, A. Whitbeck

University of Florida, Gainesville, USA

D. Acosta, P. Avery, P. Bortignon, D. Bourilkov, A. Brinkerhoff, L. Cadamuro, A. Carnes, D. Curry, R. D. Field, S. V. Gleyzer, B. M. Joshi, J. Konigsberg, A. Korytov, K. H. Lo, P. Ma, K. Matchev, H. Mei, G. Mitselmakher, D. Rosenzweig, K. Shi, D. Sperka, J. Wang, S. Wang, X. Zuo

Florida International University, Miami, USA

Y. R. Joshi, S. Linn

Florida State University, Tallahassee, USA

A. Ackert, T. Adams, A. Askew, S. Hagopian, V. Hagopian, K. F. Johnson, T. Kolberg, G. Martinez, T. Perry, H. Prosper, A. Saha, C. Schiber, R. Yohay

Florida Institute of Technology, Melbourne, USA

M. M. Baarmand, V. Bhopatkar, S. Colafranceschi, M. Hohlmann, D. Noonan, M. Rahmani, T. Roy, F. Yumiceva

University of Illinois at Chicago (UIC), Chicago, USA

M. R. Adams, L. Apanasevich, D. Berry, R. R. Betts, R. Cavanaugh, X. Chen, S. Dittmer, O. Evdokimov, C. E. Gerber, D. A. Hangal, D. J. Hofman, K. Jung, J. Kamin, C. Mills, M. B. Tonjes, N. Varelas, H. Wang, X. Wang, Z. Wu, J. Zhang

The University of Iowa, Iowa City, USA

M. Alhusseini, B. Bilki⁶⁹, W. Clarida, K. Dilsiz⁷⁰, S. Durgut, R. P. Gandrajula, M. Haytmyradov, V. Khristenko, J.-P. Merlo, A. Mestvirishvili, A. Moeller, J. Nachtman, H. Ogul⁷¹, Y. Onel, F. Ozok⁷², A. Penzo, C. Snyder, E. Tiras, J. Wetzel

Johns Hopkins University, Baltimore, USA

B. Blumenfeld, A. Cocoros, N. Eminizer, D. Fehling, L. Feng, A. V. Gritsan, W. T. Hung, P. Maksimovic, J. Roskes, U. Sarica, M. Swartz, M. Xiao, C. You

The University of Kansas, Lawrence, USA

A. Al-bataineh, P. Baringer, A. Bean, S. Boren, J. Bowen, A. Bylinkin, J. Castle, S. Khalil, A. Kropivnitskaya, D. Majumder, W. Mcbrayer, M. Murray, C. Rogan, S. Sanders, E. Schmitz, J. D. Tapia Takaki, Q. Wang

Kansas State University, Manhattan, USA

S. Duric, A. Ivanov, K. Kaadze, D. Kim, Y. Maravin, D. R. Mendis, T. Mitchell, A. Modak, A. Mohammadi, L. K. Saini

Lawrence Livermore National Laboratory, Livermore, USA

F. Rebassoo, D. Wright

University of Maryland, College Park, USA

A. Baden, O. Baron, A. Belloni, S. C. Eno, Y. Feng, C. Ferraioli, N. J. Hadley, S. Jabeen, G. Y. Jeng, R. G. Kellogg, J. Kunkle, A. C. Mignerey, S. Nabili, F. Ricci-Tam, M. Seidel, Y. H. Shin, A. Skuja, S. C. Tonwar, K. Wong

Massachusetts Institute of Technology, Cambridge, USA

D. Abercrombie, B. Allen, V. Azzolini, A. Baty, G. Bauer, R. Bi, S. Brandt, W. Busza, I. A. Cali, M. D'Alfonso, Z. Demiragli, G. Gomez Ceballos, M. Goncharov, P. Harris, D. Hsu, M. Hu, Y. Iiyama, G. M. Innocenti, M. Klute, D. Kovalskyi, Y.-J. Lee, P. D. Luckey, B. Maier, A. C. Marini, C. McGinn, C. Mironov, S. Narayanan, X. Niu, C. Paus, C. Roland, G. Roland, Z. Shi, G. S. F. Stephans, K. Sumorok, K. Tatar, D. Velicanu, J. Wang, T. W. Wang, B. Wyslouch

University of Minnesota, Minneapolis, USA

A. C. Benvenuti[†], R. M. Chatterjee, A. Evans, P. Hansen, J. Hiltbrand, Sh. Jain, S. Kalafut, M. Krohn, Y. Kubota, Z. Lesko, J. Mans, N. Ruckstuhl, R. Rusack, M. A. Wadud

University of Mississippi, Oxford, USA

J. G. Acosta, S. Oliveros

University of Nebraska-Lincoln, Lincoln, USA

E. Avdeeva, K. Bloom, D. R. Claes, C. Fangmeier, F. Golf, R. Gonzalez Suarez, R. Kamalieddin, I. Kravchenko, J. Monroy, J. E. Siado, G. R. Snow, B. Stieger

State University of New York at Buffalo, Buffalo, USA

A. Godshalk, C. Harrington, I. Iashvili, A. Kharchilava, C. Mclean, D. Nguyen, A. Parker, S. Rappoccio, B. Roozbahani

Northeastern University, Boston, USA

G. Alverson, E. Barberis, C. Freer, Y. Haddad, A. Hortiangtham, D. M. Morse, T. Orimoto, R. Teixeira De Lima, T. Wamorkar, B. Wang, A. Wisecarver, D. Wood

Northwestern University, Evanston, USA

S. Bhattacharya, J. Bueghly, O. Charaf, K. A. Hahn, N. Mucia, N. Odell, M. H. Schmitt, K. Sung, M. Trovato, M. Velasco

University of Notre Dame, Notre Dame, USA

R. Bucci, N. Dev, M. Hildreth, K. Hurtado Anampa, C. Jessop, D. J. Karmgard, N. Kellams, K. Lannon, W. Li, N. Loukas, N. Marinelli, F. Meng, C. Mueller, Y. Musienko³⁶, M. Planer, A. Reinsvold, R. Ruchti, P. Siddireddy, G. Smith, S. Taroni, M. Wayne, A. Wightman, M. Wolf, A. Woodard

The Ohio State University, Columbus, USA

J. Alimena, L. Antonelli, B. Bylsma, L. S. Durkin, S. Flowers, B. Francis, C. Hill, W. Ji, T. Y. Ling, W. Luo, B. L. Winer

Princeton University, Princeton, USA

S. Cooperstein, P. Elmer, J. Hardenbrook, S. Higginbotham, A. Kalogeropoulos, D. Lange, M. T. Lucchini, J. Luo, D. Marlow, K. Mei, I. Ojalvo, J. Olsen, C. Palmer, P. Piroué, J. Salfeld-Nebgen, D. Stickland, C. Tully, Z. Wang

University of Puerto Rico, Mayaguez, USA

S. Malik, S. Norberg

Purdue University, West Lafayette, USA

A. Barker, V. E. Barnes, S. Das, L. Gutay, M. Jones, A. W. Jung, A. Khatiwada, B. Mahakud, D. H. Miller, N. Neumeister, C. C. Peng, S. Piperov, H. Qiu, J. F. Schulte, J. Sun, F. Wang, R. Xiao, W. Xie

Purdue University Northwest, Hammond, USA

T. Cheng, J. Dolen, N. Parashar

Rice University, Houston, USA

Z. Chen, K. M. Ecklund, S. Freed, F. J. M. Geurts, M. Kilpatrick, W. Li, B. P. Padley, R. Redjimi, J. Roberts, J. Rorie, W. Shi, Z. Tu, A. Zhang

University of Rochester, Rochester, USA

A. Bodek, P. de Barbaro, R. Demina, Y. t. Duh, J. L. Dulemba, C. Fallon, T. Ferbel, M. Galanti, A. Garcia-Bellido, J. Han, O. Hindrichs, A. Khukhunaishvili, E. Ranken, P. Tan, R. Taus

Rutgers, The State University of New Jersey, Piscataway, USA

J. P. Chou, Y. Gershtein, E. Halkiadakis, A. Hart, M. Heindl, E. Hughes, S. Kaplan, R. Kunnawalkam Elayavalli, S. Kyriacou, A. Lath, R. Montalvo, K. Nash, M. Osherson, H. Saka, S. Salur, S. Schnetzer, D. Sheffield, S. Somalwar, R. Stone, S. Thomas, P. Thomassen, M. Walker

University of Tennessee, Knoxville, USA

A. G. Delannoy, J. Heideman, G. Riley, S. Spanier

Texas A& M University, College Station, USA

O. Bouhali⁷³, A. Celik, M. Dalchenko, M. De Mattia, A. Delgado, S. Dildick, R. Eusebi, J. Gilmore, T. Huang, T. Kamon⁷⁴, S. Luo, R. Mueller, D. Overton, L. Perniè, D. Rathjens, A. Safonov

Texas Tech University, Lubbock, USA

N. Akchurin, J. Damgov, F. De Guio, P. R. Duerdo, S. Kunori, K. Lamichhane, S. W. Lee, T. Mengke, S. Muthumuni, T. Peltola, S. Undleeb, I. Volobouev, Z. Wang

Vanderbilt University, Nashville, USA

S. Greene, A. Gurrola, R. Janjam, W. Johns, C. Maguire, A. Melo, H. Ni, K. Padeken, J. D. Ruiz Alvarez, P. Sheldon, S. Tuo, J. Velkovska, M. Verweij, Q. Xu

University of Virginia, Charlottesville, USA

M. W. Arenton, P. Barria, B. Cox, R. Hirosky, M. Joyce, A. Ledovskoy, H. Li, C. Neu, T. Sinthuprasith, Y. Wang, E. Wolfe, F. Xia

Wayne State University, Detroit, USA

R. Harr, P. E. Karchin, N. Poudyal, J. Sturdy, P. Thapa, S. Zaleski

University of Wisconsin - Madison, Madison, WI, USA

M. Brodski, J. Buchanan, C. Caillol, D. Carlsmith, S. Dasu, I. De Bruyn, L. Dodd, B. Gomber, M. Grothe, M. Herndon, A. Hervé, U. Hussain, P. Klabbers, A. Lanaro, K. Long, R. Loveless, T. Ruggles, A. Savin, V. Sharma, N. Smith, W. H. Smith, N. Woods

† Deceased

- 1: Also at Vienna University of Technology, Vienna, Austria
- 2: Also at IRFU, CEA, Université Paris-Saclay, Gif-sur-Yvette, France
- 3: Also at Universidade Estadual de Campinas, Campinas, Brazil
- 4: Also at Federal University of Rio Grande do Sul, Porto Alegre, Brazil
- 5: Also at Université Libre de Bruxelles, Bruxelles, Belgium
- 6: Also at University of Chinese Academy of Sciences, Beijing, China
- 7: Also at Institute for Theoretical and Experimental Physics, Moscow, Russia
- 8: Also at Joint Institute for Nuclear Research, Dubna, Russia
- 9: Also at Cairo University, Cairo, Egypt
- 10: Also at Helwan University, Cairo, Egypt
- 11: Now at Zewail City of Science and Technology, Zewail, Egypt
- 12: Also at Department of Physics, King Abdulaziz University, Jeddah, Saudi Arabia
- 13: Also at Université de Haute Alsace, Mulhouse, France
- 14: Also at Skobeltsyn Institute of Nuclear Physics, Lomonosov Moscow State University, Moscow, Russia
- 15: Also at Tbilisi State University, Tbilisi, Georgia
- 16: Also at CERN, European Organization for Nuclear Research, Geneva, Switzerland
- 17: Also at RWTH Aachen University, III. Physikalisches Institut A, Aachen, Germany
- 18: Also at University of Hamburg, Hamburg, Germany
- 19: Also at Brandenburg University of Technology, Cottbus, Germany
- 20: Also at Institute of Physics, University of Debrecen, Debrecen, Hungary
- 21: Also at Institute of Nuclear Research ATOMKI, Debrecen, Hungary
- 22: Also at MTA-ELTE Lendület CMS Particle and Nuclear Physics Group, Eötvös Loránd University, Budapest, Hungary
- 23: Also at Indian Institute of Technology Bhubaneswar, Bhubaneswar, India
- 24: Also at Institute of Physics, Bhubaneswar, India
- 25: Also at Shoolini University, Solan, India
- 26: Also at University of Visva-Bharati, Santiniketan, India
- 27: Also at Isfahan University of Technology, Isfahan, Iran
- 28: Also at Plasma Physics Research Center, Science and Research Branch, Islamic Azad University, Tehran, Iran
- 29: Also at Università degli Studi di Siena, Siena, Italy
- 30: Also at Scuola Normale e Sezione dell'INFN, Pisa, Italy
- 31: Also at Kyung Hee University, Department of Physics, Seoul, Korea
- 32: Also at International Islamic University of Malaysia, Kuala Lumpur, Malaysia
- 33: Also at Malaysian Nuclear Agency, MOSTI, Kajang, Malaysia
- 34: Also at Consejo Nacional de Ciencia y Tecnología, Mexico City, Mexico
- 35: Also at Warsaw University of Technology, Institute of Electronic Systems, Warsaw, Poland
- 36: Also at Institute for Nuclear Research, Moscow, Russia
- 37: Now at National Research Nuclear University 'Moscow Engineering Physics Institute' (MEPhI), Moscow, Russia
- 38: Also at St. Petersburg State Polytechnical University, St. Petersburg, Russia
- 39: Also at University of Florida, Gainesville, USA
- 40: Also at P.N. Lebedev Physical Institute, Moscow, Russia
- 41: Also at California Institute of Technology, Pasadena, USA
- 42: Also at Budker Institute of Nuclear Physics, Novosibirsk, Russia
- 43: Also at Faculty of Physics, University of Belgrade, Belgrade, Serbia
- 44: Also at INFN Sezione di Pavia^a, Università di Pavia^b, Pavia, Italy
- 45: Also at University of Belgrade, Belgrade, Serbia
- 46: Also at National and Kapodistrian University of Athens, Athens, Greece
- 47: Also at Riga Technical University, Riga, Latvia

- 48: Also at Universität Zürich, Zurich, Switzerland
49: Also at Stefan Meyer Institute for Subatomic Physics (SMI), Vienna, Austria
50: Also at Istanbul Aydin University, Istanbul, Turkey
51: Also at Mersin University, Mersin, Turkey
52: Also at Piri Reis University, Istanbul, Turkey
53: Also at Gaziosmanpasa University, Tokat, Turkey
54: Also at Adiyaman University, Adiyaman, Turkey
55: Also at Ozyegin University, Istanbul, Turkey
56: Also at Izmir Institute of Technology, Izmir, Turkey
57: Also at Marmara University, Istanbul, Turkey
58: Also at Kafkas University, Kars, Turkey
59: Also at Istanbul University, Faculty of Science, Istanbul, Turkey
60: Also at Istanbul Bilgi University, Istanbul, Turkey
61: Also at Hacettepe University, Ankara, Turkey
62: Also at Rutherford Appleton Laboratory, Didcot, UK
63: Also at School of Physics and Astronomy, University of Southampton, Southampton, UK
64: Also at Monash University, Faculty of Science, Clayton, Australia
65: Also at Bethel University, St. Paul, USA
66: Also at Karamanoğlu Mehmetbey University, Karaman, Turkey
67: Also at Utah Valley University, Orem, USA
68: Also at Purdue University, West Lafayette, USA
69: Also at Beykent University, Istanbul, Turkey
70: Also at Bingol University, Bingol, Turkey
71: Also at Sinop University, Sinop, Turkey
72: Also at Mimar Sinan University, Istanbul, Istanbul, Turkey
73: Also at Texas A&M University at Qatar, Doha, Qatar
74: Also at Kyungpook National University, Daegu, Korea